

DTIC FILE COPY

# NAVAL POSTGRADUATE SCHOOL

## Monterey, California

AD-A225 329



DTIC  
ELECTE  
AUG 17 1990  
S B D  
Go

## THESIS

PHYSICAL PROCESSES IN HOLLOW CATHODE DISCHARGE

by

Han, Hwang-Jin

December 1989

Thesis Advisor:

Richard C. Olsen

Approved for public release: distribution is unlimited

00 08 15 152

## REPORT DOCUMENTATION PAGE

1a. REPORT SECURITY CLASSIFICATION <b>Unclassified</b>			1b. RESTRICTIVE MARKINGS		
2a. SECURITY CLASSIFICATION AUTHORITY			3. DISTRIBUTION / AVAILABILITY OF REPORT <b>Approved for public release; distribution is unlimited</b>		
2b. DECLASSIFICATION / DOWNGRADING SCHEDULE					
4. PERFORMING ORGANIZATION REPORT NUMBER(S)			5. MONITORING ORGANIZATION REPORT NUMBER(S)		
6a. NAME OF PERFORMING ORGANIZATION <b>Naval Postgraduate School</b>		6b. OFFICE SYMBOL (If applicable) <b>61</b>	7a. NAME OF MONITORING ORGANIZATION <b>Naval Postgraduate School</b>		
6c. ADDRESS (City, State, and ZIP Code) <b>Monterey, California 93943-5000</b>			7b. ADDRESS (City, State, and ZIP Code) <b>Monterey, California 93943-5000</b>		
8a. NAME OF FUNDING / SPONSORING ORGANIZATION		8b. OFFICE SYMBOL (If applicable)	9. PROCUREMENT INSTRUMENT IDENTIFICATION NUMBER		
8c. ADDRESS (City, State, and ZIP Code)			10. SOURCE OF FUNDING NUMBERS		
			PROGRAM ELEMENT NO.	PROJECT NO.	TASK NO.
			WORK UNIT ACCESSION NO.		
11. TITLE (Include Security Classification) <b>Physical Processes in Hollow Cathode Discharge</b>					
12. PERSONAL AUTHOR(S)					
13a. TYPE OF REPORT <b>Master' Thesis</b>		13b. TIME COVERED FROM _____ TO _____		14. DATE OF REPORT (Year, Month, Day) <b>1989 December</b>	
				15. PAGE COUNT <b>61</b>	
16. SUPPLEMENTARY NOTATION <b>The views expressed in this thesis are those of the author and do not reflect the official policy or position of the Department of Defense or the U. S. Government</b>					
17. COSATI CODES			18. SUBJECT TERMS (Continue on reverse if necessary and identify by block number)		
FIELD	GROUP	SUB-GROUP	<b>Hollow Cathodes (physics), Plasma Source, Ion Beams, Source theses,</b>		
19. ABSTRACT (Continue on reverse if necessary and identify by block number) <b>The hollow cathode is an effective source of dense, low energy plasma. Hollow cathodes find use in ion beam sources for laboratory and space applications. They can also be used independently for satellite charge control, and ion beam neutralization. A heaterless hollow cathode design was tested with argon gas used as a propellant. This thesis work investigated the device properties, that is, the emission currents as a function of discharge current, propellant flow rate and other physical parameters. Starting behavior was a main point of the investigation. The results of these experiments were compared with studies of the conventional hollow cathode.</b> <i>Keywords:</i>					
20. DISTRIBUTION / AVAILABILITY OF ABSTRACT <input checked="" type="checkbox"/> UNCLASSIFIED/UNLIMITED <input type="checkbox"/> SAME AS RPT <input type="checkbox"/> DTIC USERS			21. ABSTRACT SECURITY CLASSIFICATION <b>Unclassified</b>		
22a. NAME OF RESPONSIBLE INDIVIDUAL <b>Professor Richard Christopher Olsen</b>			22b. TELEPHONE (Include Area Code) <b>(408) 646 - 2019</b>		22c. OFFICE SYMBOL <b>61 0s</b>

Approved for public release; distribution is unlimited.

Physical Processes in Hollow Cathode Discharge Sources

by

Han, Hwang-Jin  
Major, Republic of Korea Army  
B.S., Republic of Korea Military Academy, 1981

Submitted in partial fulfillment of the  
requirements for the degree of

MASTER OF SCIENCE IN PHYSICS

from the

NAVAL POSTGRADUATE SCHOOL  
December 1989

Author:

*J. Han, J. Hwang-jin*  
Han, Hwang-Jin

Approved by:

*Richard Christopher Olsen*  
Richard C. Olsen, Thesis Advisor

*S. Gnalingam*  
S. Gnalingam, Second Reader

*Karlheinz E. Woehler*  
Karlheinz E. Woehler, Chairman  
Department of Physics

## ABSTRACT

The hollow cathode is an effective source of dense, low energy plasma. Hollow cathodes find use in ion beam sources for laboratory and space applications. They can also be used independently for satellite charge control, and ion beam neutralization. A heaterless hollow cathode design was tested with argon gas used as the propellant. This thesis work investigated the device properties, that is, the emission currents as a function of discharge current, propellant flow rate and other physical parameters. Starting behavior was a main point of the investigation. The results of these experiments were compared with studies of the conventional hollow cathode.

Accession For	
NTIS GRA&I	<input checked="checked" type="checkbox"/>
DTIC TAB	<input type="checkbox"/>
Unannounced	<input type="checkbox"/>
Justification	
By _____	
Distribution/	
Availability Codes	
Dist	Avail and/or Special
A-1	



## TABLE OF CONTENTS

I.	INTRODUCTION	1
II.	BACKGROUND	4
	A. HOLLOW CATHODE PHYSICS	4
	B. PREVIOUS EXPERIMENTAL RESULTS	7
	C. HEATERLESS HOLLOW CATHODE	18
III.	EXPERIMENTAL EQUIPMENT AND PROCEDURE	25
	A. EXPERIMENTAL EQUIPMENT	25
	1. Discharge Chamber	25
	2. Electrical Circuit	26
	3. Measuring Equipment	29
	4. Vacuum System	29
	B. PROCEDURE	29
	1. Vacuum System	29
	2. Starting and Shutting Down the Plasma	
	Source	31
	(A). Standard Hollow Cathode	31
	(B). Spectra-Mat Hollow Cathode	33
IV.	EXPERIMENTAL RESULTS	34
	A. STANDARD HOLLOW CATHODE	34
	1. Flow Rate Dependence	34
	2. Temperature Dependence	34
	3. Time Dependence	36

B.	SPECTRA-MAT HOLLOW CATHODE	38
1.	Idle Mode Discharge	38
2.	Extraction of Discharge	40
3.	Discharge Failure	41
V.	CONCLUSION	46

## LIST OF TABLES

Table 2.1	Values of Coefficients A and B for various gases	21
Table 2.2	Mininum Sparking Potentials	21
Table 4.1	Data for Spectra-Mat Cathode	40

## LIST OF FIGURES

Fig. 1.1	Hollow Cathode Schematic	2
Fig. 2.1	Discharge Initiation Data for Cathode with Rolled Foil Dispenser	9
Fig. 2.2	Small Orificed Hollow Cathode	10
Fig. 2.3	Variation of Minimum Discharge Voltage with Pressure for Several Separations	13
Fig. 2.4	Keeper Voltage Dependence on the Operation Time	14
Fig. 2.5	Keeper Voltage Dependence on the Mass Flow Rate	14
Fig. 2.6	Volt Ampere Discharge Characteristics of Cesium Hollow Cathode for Different Flow Rate	15
Fig. 2.7	Comparison between D.C. Ignition Voltage and Pulse Ignition Voltage	17
Fig. 2.8	Relation between Pulse Ignition Voltage and Mercury Flow Rate	17
Fig. 2.9	Entire Test Log of the Cathode	18
Fig. 2.10	Paschen's Law (Breakdown voltage $V_b$ as a function of the reduced electrode distance $P \cdot D$ )	20
Fig. 2.11	Spectra-Mat Hollow Cathode Apparatus	24
Fig. 3.1	General Experimental Arrangement	25



Fig. 3.2	Electrical Circuitry for the HC-252 Hollow Cathode	27
Fig. 3.3	Electrical Circuitry for the Spectra-Mat Hollow Cathode	28
Fig. 3.4	Major Parts of Varian Vacuum System	30
Fig. 3.5	Relation between Propellant Flow Rate and Chamber Pressure	30
Fig. 4.1	Discharge Voltage vs Flow Rate	35
Fig. 4.2	Discharge Voltage vs Heater Current	36
Fig. 4.3	Idle Mode Discharge Current vs Keeper Biasing Potential( $V_k$ )	37
Fig. 4.4	Idle Mode Discharge Current for Different Flow Rates	39
Fig. 4.5	Idle Mode Discharge Current for Different Biasing Keeper Voltage	39
Fig. 4.6	Picture of Damaged Cathode Surface	43
Fig. 4.7	Broken Tip of Ceramic Insulator	44
Fig. 4.8	Detailed Diagram of Disassembled Spectra-Mat Hollow Cathode	45

## ACKNOWLEDGEMENTS

I wish to express my gratitude and appreciation to thesis advisor, Professor Richard Christopher Olsen and second reader, Professor S. Gnanalingam for the instruction, guidance and friendly advices throughout this study.

I wish to thank the numerous scientists who contributed figures and data for this work, particularly, Dr. Paul J. Wilbur and Dr. Daniel E. Siegfried, Colorado State University.

Finally, many thanks to my wife, Kyoung-Sook and my son, Frederick Teut, for their love and being supportive for two and half years in Monterey, California.

## I. INTRODUCTION

One motivation for the study of gas discharge technology is to produce a plasma for ion beams in laboratory and space applications. One popular and reliable implementation is the hollow cathode. Hollow cathode gas discharge devices provide an important capability as a source of low energy plasma. Applications include the electron source for the discharge chamber in ion bombardment thrusters and the neutralizer for ion thruster beams. Ion thrusters, developed for space applications, are finding increasing use in vacuum processing applications. Large area ion beams are extracted from electron bombardment-type ion sources whose ionizing electrons are typically supplied by a hot refractory metal filament cathode. However, short filament lifetimes (several tens of hours), difficulties in maintaining constant filament electron emission, and filament breakage, are significant undesirable features of using this type of cathode in space flight or production processing equipment.

Hollow cathodes offer substantially longer lifetimes than filament cathodes. However, cathodes are intrinsically complex devices and for a specific application require a great deal of testing and parametric optimization before reliable operation can be assured. These technical challenges have limited their application in industrial ion sources. Fig. 1.1 details a hollow cathode which does operate reliably, is easy to fabricate, has demonstrated long life operation, and may be used for ion beam and plasma sources. [Ref. 2]

The hollow cathode consists of an outer refractory metal tube, usually tantalum, covered on its downstream end by an orifice plate usually made of

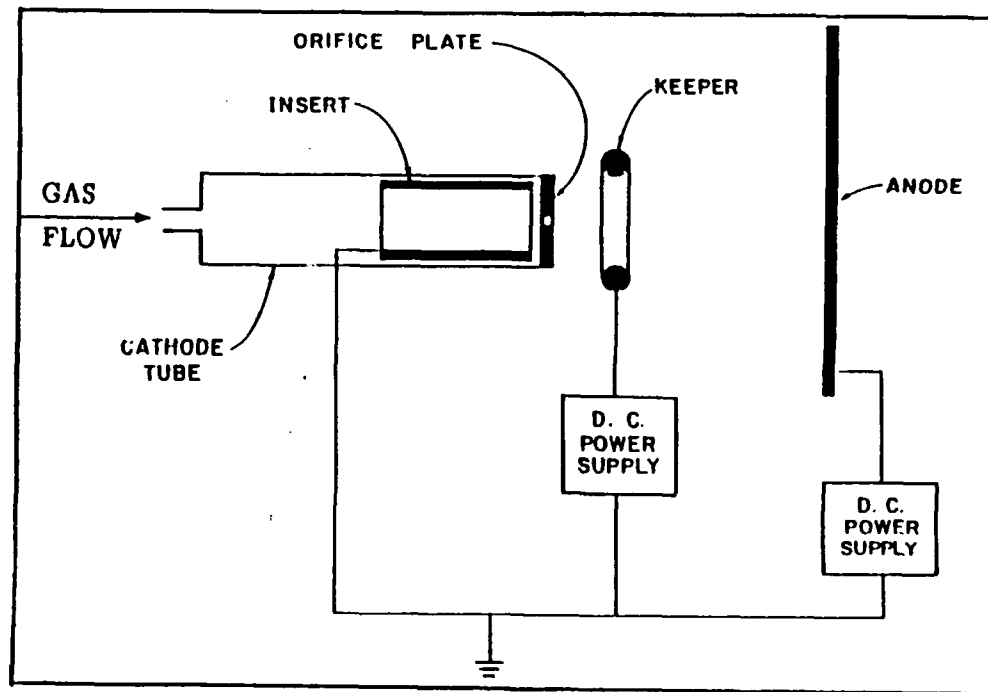


Fig. 1.1 Hollow Cathode Schematic

thoriated tungsten. The cathode also normally incorporates a refractory metal insert either coated or impregnated with such chemicals as barium compounds, which aid the emission process by reducing the work function of the insert surface. The cathodes used in ion thrusters typically have inner diameters of a few millimeters and orifice diameters of a few tenths to one millimeter. The insert length is usually a few tube diameters. The electron current is collected by an anode biased positive with respect to the cathode. Hollow cathodes generally utilize a small secondary anode, called a keeper, which is used to initiate the discharge. A heater is normally used to heat the cathode as an aid to starting the emission process. However, the discharge is self-sustaining (self-heating) once established and the heater can be turned off or turned down.

As mentioned above, there has been an interest in hollow cathodes for use in ion bombardment thrusters as the electron source for the discharge chamber and as the neutralizer for the thruster beam. Because operating requirements for the thruster dictate long lifetimes and stable operation for this component, it has become of prime importance to understand physical phenomena taking place in the hollow cathodes used in these devices.

With the realization that electric propulsion systems will probably be applied at first to the station keeping mission, it has become apparent that the ability to operate a thruster without deterioration for thousands of hours is no longer sufficient. It must also be capable of rapidly starting from cold thousands of times, and it is therefore important to identify the parameters governing this process, so that problem areas can receive attention. In the case of the electron bombardment thruster, the ability to initiate the discharge on demand is largely dependent on the hollow cathode. For this reason, this aspect of hollow cathode operation has been studied in conjunction with the fundamental investigations mentioned above.

In this investigation, it was found that such characteristics are more complex than was thought initially from consideration of other gaseous breakdown phenomena. In particular, under any one set of conditions, the initiation voltage required was not reproducible, but fell within a range, the magnitude of which depended strongly on temperature and flow rate. In deciding upon suitable initiation parameters it is therefore necessary to balance these quantities. [Ref. 6]

The objective of this study has been to gain a better insight into the physical process of hollow cathode operation. Towards this goal, an experimental investigation was undertaken to measure plasma properties and other pertinent physical parameters, and to observe the starting behavior under several conditions.

## II. BACKGROUND

### A. HOLLOW CATHODE PHYSICS

Ignition of the standard hollow cathode begins with the activation of the heater power supply, which heats the cathode to approximately 1000°C, followed by the introduction of propellant into the cathode as shown in Fig. 1.1. The keeper supply is then activated, the gas breaks down electrically and an arc discharge ignites. Stable hollow cathode arcs require a copious source of electrons which the insert provides by the mechanism of field enhanced thermionic emission. In this scenario, the insert must be heated to a temperature of approximately 1000°C over a region large enough such that in combination with the electric field generated by a nearby, dense plasma, the insert emits enough electrons to maintain a stable arc. [Ref. 10]

Daniel E. Siegfried, Colorado State University, provided the current understanding of the physical processes which take place inside the hollow cathode. He explained as follows in "Phenomenological Model Describing Orificed, Hollow Cathode Operation". [Ref. 7]

The cathode orifice maintains a high neutral density inside the cathode by restricting the propellant flow and it also provides a current path to the downstream discharge. The electron emission comes uniformly from a narrow ( $\approx 2\text{mm}$ ) band on the downstream end of the insert. The electrons are produced at the surface of the insert by field-enhanced, thermionic emission (the very strong electric field is a consequence of a very dense plasma and the resulting potential drop across a very thin plasma sheath). The electrons produced at the insert surface are accelerated across the plasma sheath by a potential of 8 to 10 volts. Since the mean free path for inelastic collisions of these energetic electrons is on the order of the internal cathode diameter, the "ion production" region can be idealized to be the volume circumscribed by the emitting region of the insert. The dense internal plasma is established by the ionization taking place in this region. Ions produced in this volume diffuse

out of it at the Bohm velocity. The electrons strike the insert surface with sufficient energy to heat it to the temperature necessary to provide the required electron emission. The emission surface temperature, however, is determined not only by the emission current but also by the local plasma properties.

The plasma properties in the ion production region are coupled into the problem by the energy balance at the insert surface in the following manner. The plasma properties determine the ion flux and therefore the energy input to the emission surface. For a given emission current, the surface temperature is determined by the energy balance which demands that the thermal losses from the surface due to electron production, radiation and conduction are balanced by the energy input from the ion flux. The plasma properties also affect the required emission temperature because they determine the magnitude of the electric field—enhancement in the emission process. Therefore, for a given emission current the surface temperature and plasma properties must be consistent to the extent that they satisfy the energy balance at the surface. All cathode surfaces which contact the plasma receive ion currents proportional to the Bohm velocity and the plasma density adjacent to the surface. Electron emission, on the other hand, can be assumed to come only from the 2mm band on the downstream end of the insert. The total emission current from the cathode is equal to the sum of the ion currents to the various cathode surfaces and the current of the emitted electrons.

Certain aspects of this phenomenological model can be expressed analytically in a simple form which will allow comparison with experimental results. The plasma density adjacent to a particular surface ( $n$ ) can be calculated based on the Bohm condition using

$$n = \frac{j_i}{ev B_{ohm}} = \frac{I_i}{Ae \left[ \frac{KT_e}{m_e} \right]^{1/2}} \quad (2.1)$$

where  $I_i$  is the ion current to the surface,  $A$  is the surface area,  $T_e$  is the Maxwellian electron temperature ( $^{\circ}K$ ), and  $K$  is Boltzmann's constant. For an electron emitting surface the measured current to the surface is determined by both collected ions and emitted electrons, so that the total current density to the surface is

$$j_{total} = j_i + j_e \quad (2.2)$$

where  $j_i$  is the ion current density and  $j_e$  is the electron emission current density. The ratio of ion to electron currents can be estimated from an energy balance on the emitting surface. In such a balance the ion heating power is equated to power conducted and radiated from the surface plus the power required to boil off electrons. The equation describing this is

$$j_e \bar{\phi} + q = j_i (V_c + V_i - \phi_s) \quad (2.3)$$

where  $\bar{\phi}_e$  is the effective work function of the surface,  $q$  is the thermal heat flux away from the surface,  $V_c$  is the potential drop across the plasma sheath,  $V_i$  is the ionization potential, and  $\phi_s$  is the work function of the surface material (a material property). Equation (2) and (3) can be combined to give the electron emission current density from the surface,

$$j_e = \frac{j_{total} - aq}{1 + a\bar{\phi}_e} \quad (2.4)$$

where  $a \equiv (V_c + V_i - \phi_s)^{-1}$ . In general the thermal loss is a function of the surface temperature and the cathode thermal design. Most of the thermal loss is due to radiation from the outer surface of the insert to rather cold external surfaces, and can be estimated from

$$q \cong \epsilon \sigma T^4 \quad (2.5)$$

where  $\epsilon$  is the emissivity ( $\cong 0.5$  for tantalum),  $\sigma$  is the Stefan-Boltzmann constant, and  $T$  is the surface temperature. Emission from the surface is assumed to be given by the Schottky equation for field-enhanced, thermionic emission

$$j_e = A_0 T^2 \exp \left[ -\frac{e\bar{\phi}_e}{KT} \right] \quad (2.6)$$

where  $A_0 = 120 \text{ A/cm}^2\text{K}^2$  and the other parameters are as previously defined.

The average effective work function  $\bar{\phi}_e$  is given by

$$\bar{\phi}_e = \phi_s - \left[ \frac{e|E|}{4\pi\epsilon_0} \right]^{-\frac{1}{2}} \quad (2.7)$$

where  $\epsilon_0$  is the permittivity of free space and  $E$ , the electric field adjacent to the surface, can be estimated using

$$E = -\frac{dV}{dx} = -\frac{4}{3} \frac{V_c}{\lambda_D} = -\frac{4}{3} V_c \left[ \frac{ne^2}{\epsilon_0 KT_e} \right]^{-\frac{1}{2}} \quad (2.8)$$

Here the factor of  $4/3$  comes from Child's Law considerations and the sheath thickness is estimated as one Debye length ( $\lambda_D$ ). [Ref. 16]



This model provides an estimate of the insert temperature and this is a critical parameter in determining both the cathode lifetime and performance. This can be done for example, by picking an electron temperature and the plasma potential. These properties have been measured experimentally and found to be rather insensitive to operating conditions with typical values of  $-0.8$  eV and  $\cong 8.0$  volts respectively for a cathode operating at a few amperes of discharge current. Using these values together with a specified surface work function ( $\phi_s$ ) and the desired emission current ( $j_{\text{total}}$ ), Equations (1) through (8) can be solved to provide the emission surface temperature ( $T$ ). Note that the solution scheme would generally be an iterative one requiring an initial guess of a value for either  $j_e$  or  $T$ . Typical results are:  $T = 1000^\circ\text{C}$ . [Ref. 7]

## B. PREVIOUS EXPERIMENTAL RESULTS

Much of the published work on standard hollow cathode in the 1970's and 1980's was done at Colorado State University, as illustrated by the work of Siegfried [Ref. 3,7,8] and Williams [Ref. 31,32,33,34]. This work was concerned with the physical phenomena inside the hollow cathode. As part of this thesis work, a determined search for other experimental results was made. The initial work in the United States was done, or sponsored by, NASA Lewis Research Center in the 1960's. [Ref. 17,35,36] During this decade, parametric characteristics of the hollow cathode were closely observed and described.

Many similar investigations with hollow cathodes have been conducted by other countries — England [Ref. 5,6,13,14,20,22,23,24,25,26], Germany [Ref. 21,27], U.S.S.R. [Ref. 19], China [Ref. 28] and Japan. [Ref. 29,30]

## 1. England

Work by the Royal Aerospace Establishment(RAE) and at Mullard Laboratory, provides a comprehensive look at behavior of hollow cathode discharges, with a variety of cathode geometries. This investigation considered starting behavior as a function of temperature, flow rate, voltage, geometry of the orifice and dispenser, and barium availability. Discharge initiation experiments using the keeper electrode were done for a tubular insert cathode, a rolled foil dispenser cathode, a curved orificed cathode and non-bariated cathode design. For a given cathode and fixed flow rate and temperature, the voltage necessary to start a discharge falls randomly between two limits. Above the upper limit, a discharge will always occur, while below the lower limit one can never be obtained. As temperature and flow rate are increased, these limits approach each other until at sufficiently high values, they merge and behavior becomes reproducible. In the design of a thruster system, it is desirable to choose these parameters so that the upper limit is always exceeded from these studies. Fig. 2.1 shows one typical result. [Ref. 6]

Further experiments at RAE provide basic information on the physical processes operating in cathodes. The basic design features of this hollow cathode are illustrated in Fig. 2.2. The cathode tip was a tungsten disk (1mm thick and 3.5mm diameter) electron-beam welded into a tantalum tube. It was provided with a central orifice of between 100 and 350 $\mu$ m diameter formed by either spark erosion or diamond drilling. A stainless-steel flange at the upstream end of the cathode was provided for mating with other components.

To initiate the discharge a keeper was used. This consisted of a thin molybdenum disk with a 2mm central hole, and it was spaced about 1mm from the

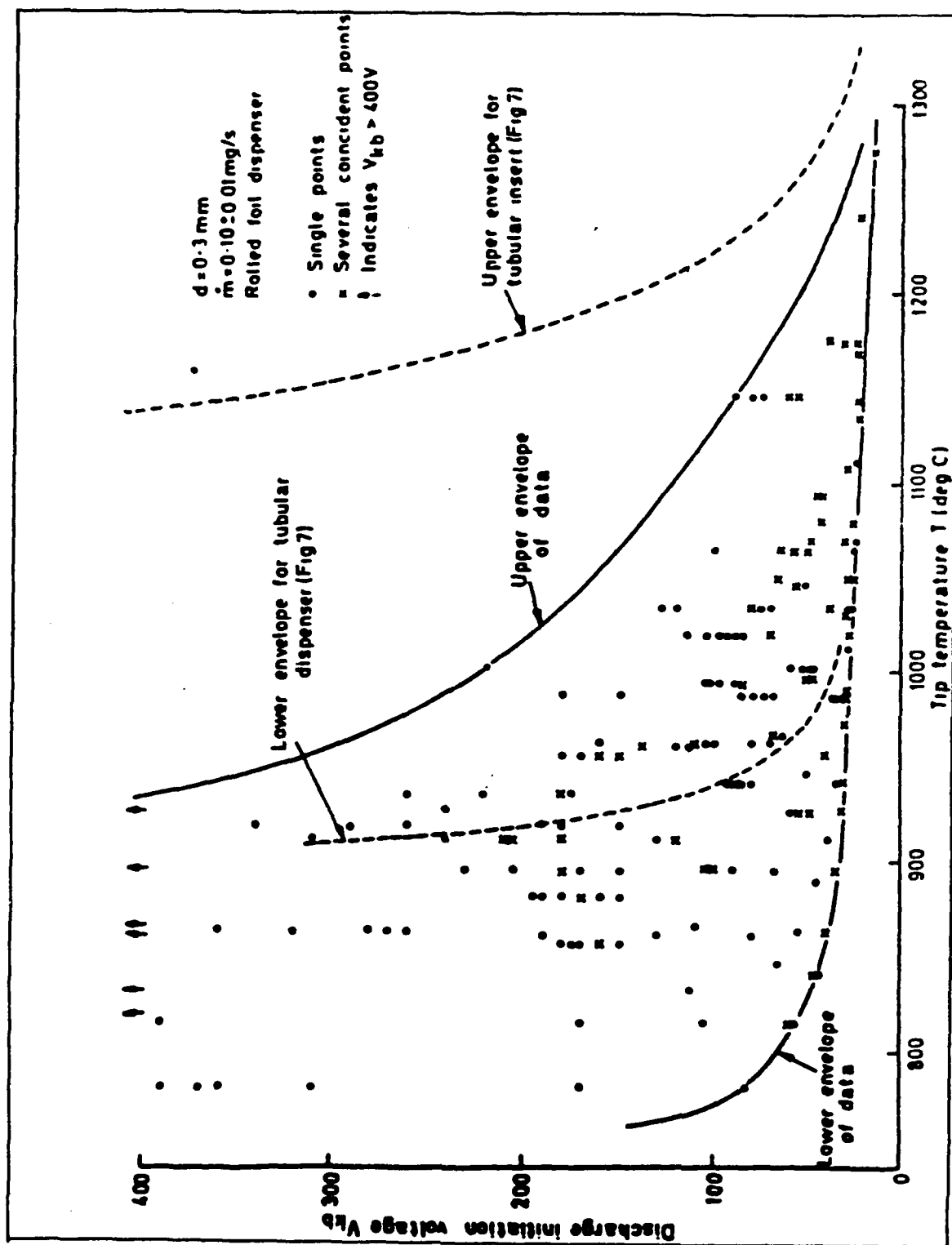


Fig. 2.1 Discharge Ignition Data for Cathode with Rolled Foil Dispenser [Ref.6]

cathode tip. The anode, or beam simulator electrode, was normally a disk of stainless steel whose distance from the cathode could be varied.

From the result of these experiments, the following physical explanation of hollow cathode behavior can be deduced. The results obtained suggest certain emission mechanisms that may account for the observed behavior. It seems certain that thermionic emission is normally necessary to initiate the discharge from this form of hollow cathode, but the site of this emission was not established. However, modification to include an internal auxiliary electrode showed that starting by field emission is quite feasible, even in the absence of electron-emitting coatings. Thus, thermionic emission is not always required.

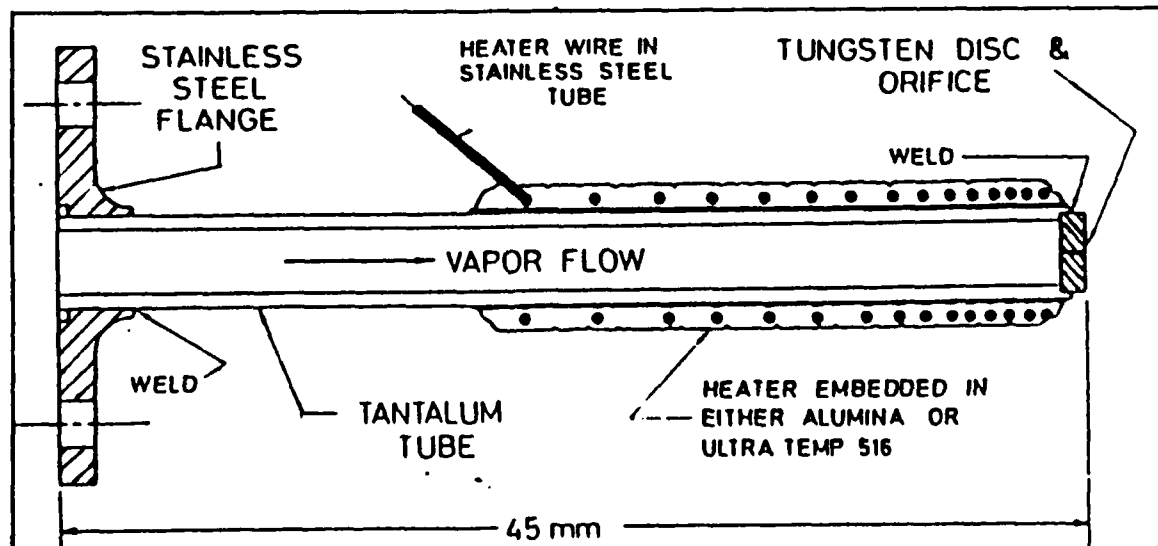


Fig. 2.2 Small-Orificed Hollow Cathode

Once breakdown has occurred and a current is drawn to the anode, thermionic emission cannot possibly account for the high current densities obtained. One possibility is field-enhanced emission caused by sufficiently high electric fields across the space charge sheath separating the walls of the cathode from an internal

plasma. This effect was shown by Schottky to be due to a reduction in the surface potential barrier. This is produced by the external accelerating field so that the work function is decreased and the emission thus increased. Analysis shows that if an electric field  $E$  is applied to an emitter the work function is reduced by an amount  $(eE/4\pi\epsilon_0)^{1/2}$ , where  $e$  is the electron charge. It follows therefore that if  $I_s$  is the saturated emission current obtained without an external field and  $I_s'$  is the saturated current with an external field  $E$  then

$$I_s' = I_s \frac{\exp(eE/4\pi\epsilon_0)^{1/2}}{KT} \quad (2.9)$$

This is the Schottky equation of field emission. [Ref. 37]

The conditions within the hollow cathode are unknown, but it is possible that  $T$  will be close to the value measured outside ( $4 \times 10^3$  °K) and that  $n_e$  will be much higher owing to the larger pressure and the presence of barium. Taking  $n_e \cong 10^{13} \text{ cm}^{-3}$  and assuming that the sheath is of the order of a Debye length  $\lambda_D$  where

$$\lambda_D = \left[ \frac{KT_e}{4\pi n_e e^2} \right]^{1/2} \quad (2.10)$$

Then  $\lambda_D \cong 10^{-4} \text{ cm}$  and the electric field gradient  $G \cong 4 \times 10^4 \text{ V/cm}$  for a plasma potential of 5V. This results from a large increase in the ion density in the sheath at the negative electrode, probably to values several orders of magnitude greater than the prevailing ion density in the plasma. [Ref. 14]

Another emission mechanism that could be very effective in the hollow cathode is the release of electrons by the impact of excited atoms. High yields are

to be expected when the excitation energies are not much greater than the work function of the emitting surface. Excited propellant atoms can be formed by a number of processes in the discharge, such as collisional excitation or charge transfer, provided that the electron-neutral and ion-neutral mean free paths are less than a typical orifice dimension. By considering the emission and absorption of resonance radiation, von Engel and Robson showed that it is probable that all of the atoms back-scattered toward the cathode by collisions with ions reach a small area of the cathode surface in excited states and thus cause electron emission. [Ref. 14]

This emission mechanism, therefore, is capable of providing the required current density, and further evidence for its existence is provided by the ability of stable spot mode discharges to operate at potentials considerably lower than the ionization potential of the propellant(mercury). From Fig. 2.3, it can be seen that the minimum discharge voltage approached a value close to 6V as the pressure was increased. This corresponds to the maximum of the cross section for excitation of mercury atoms to the 4.9 eV metastable level, and these are very effective at producing emission. [Ref. 14]

It will be noted that the preceding mechanism is not in any way dependent on the presence of an alkali metal within the cathode, and it should therefore operate successfully in the absence of the triple carbonate coating. It was, in fact, found that a discharge could be run without this coating, but the voltage required was considerably higher than normal. This suggests that a mechanism requiring the coating normally operated in conjunction with that dependent on metastable atoms.

The hollow cathode mechanism is undoubtedly more complex than the preceding treatment would suggest. Although it seems likely that, in some cases, either or both of the emission processes discussed so far are dominant, others may be necessary to explain all of the data satisfactory. [Ref. 14]

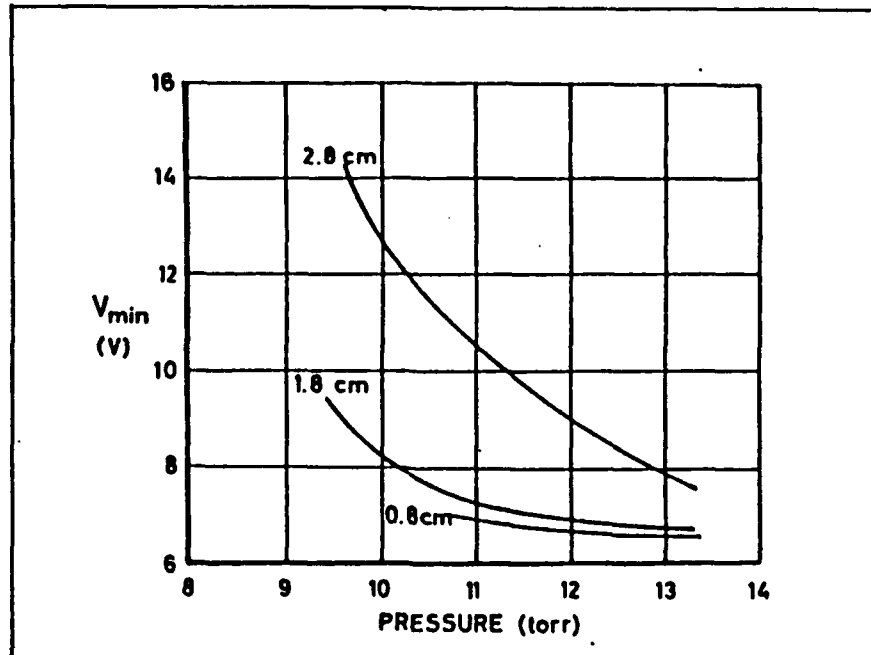


Fig. 2.3 Variation of Minimum Discharge Voltage with Pressure for Several Separations. [Ref. 14]

## 2. Germany

The research work on hollow cathodes as plasma bridge neutralizers for ion thrusters started at the University of Giessen at 1970. S.E Walther, K.H. Groh and H.W. Loeb were concerned about the life time of the cathodes. Duration tests with oxide coated rolled-foil inserts showed an increase of the keeper voltage with increasing operation time. A neutralizer system with impregnated insert was investigated in a shortened duration test of about 1,000 hours including some ignitions after exposure to air. The result is graphed in Fig. 2.4. The keeper voltage raises rapidly in the first 100 hours from 18 to 20 volts and then remains constant at about 20 volts. The keeper current is fixed at 0.3 ampere. Moreover, the dependence of the keeper voltage on the mass flow rate was

recorded after 1,000 hours operation as shown in Fig. 2.5. The curve got flatter, resulting in lower keeper voltages at very small mass flow rates. [Ref. 27]

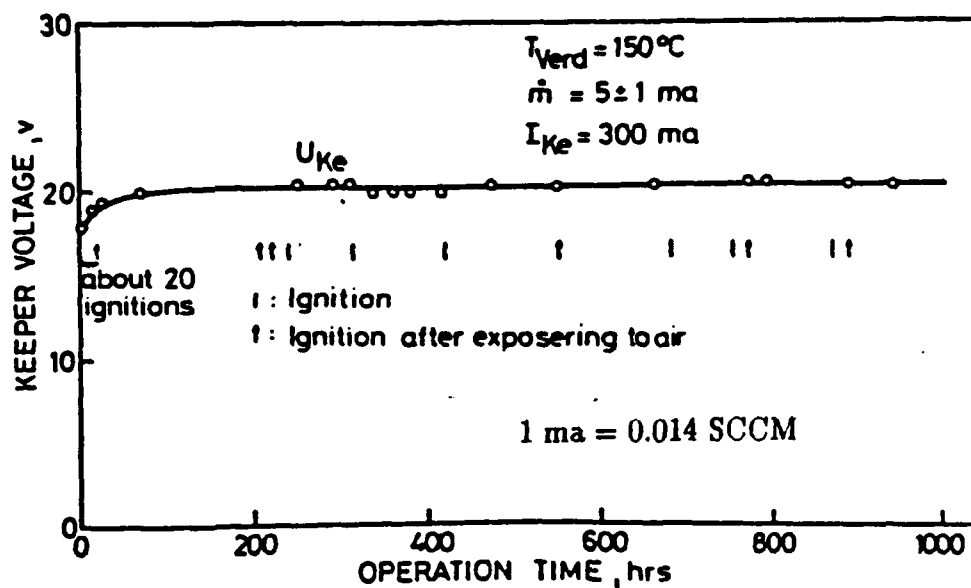


Fig. 2.4 Keeper Voltage Dependence on the Operation time [Ref. 27]

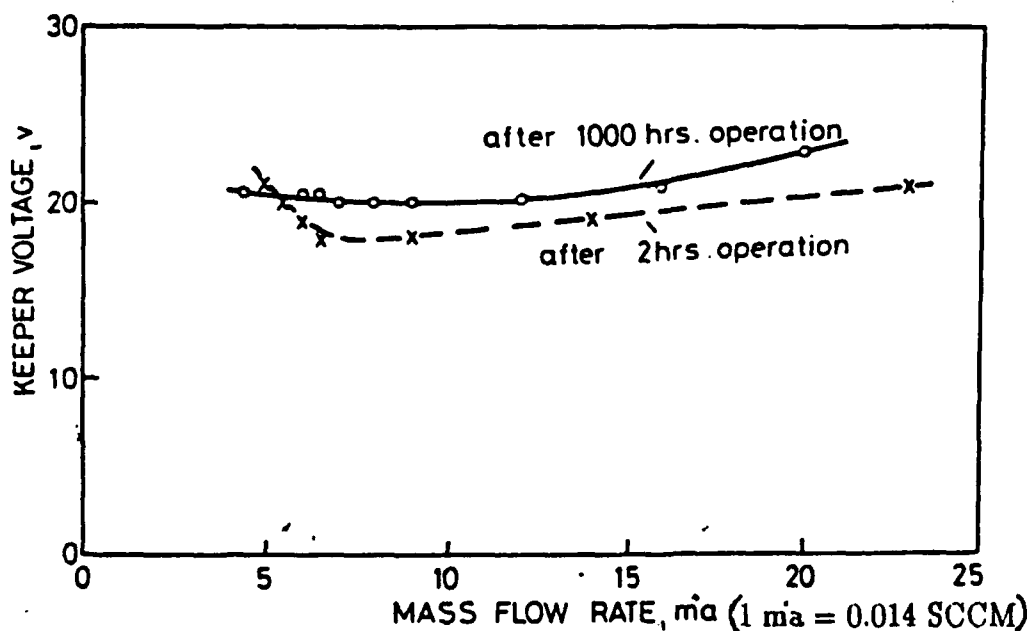


Fig. 2.5 Keeper Voltage Dependence on the Mass Flow Rate [Ref. 27]



### 3. U.S.S.R

In 1988, parametric investigation of the hollow cathode for ion thrusters was presented in the U.S.S.R. This paper presented the result of parametric investigations of a cesium hollow cathode with diameter of 5 mm. Fig. 2.6 shows typical voltage-current characteristics of the discharge. Saturation of current is seen under the different mass flow rates. Appearance of abnormal resistance in a discharge gap can be predicted as follows;

- emission current limitation as a result of a virtual cathode in a discharge gap;

- discharge current limitation as a result of the lack of discharge carrier at an anode surface and a positive anode decrease of potential [Ref. 19]

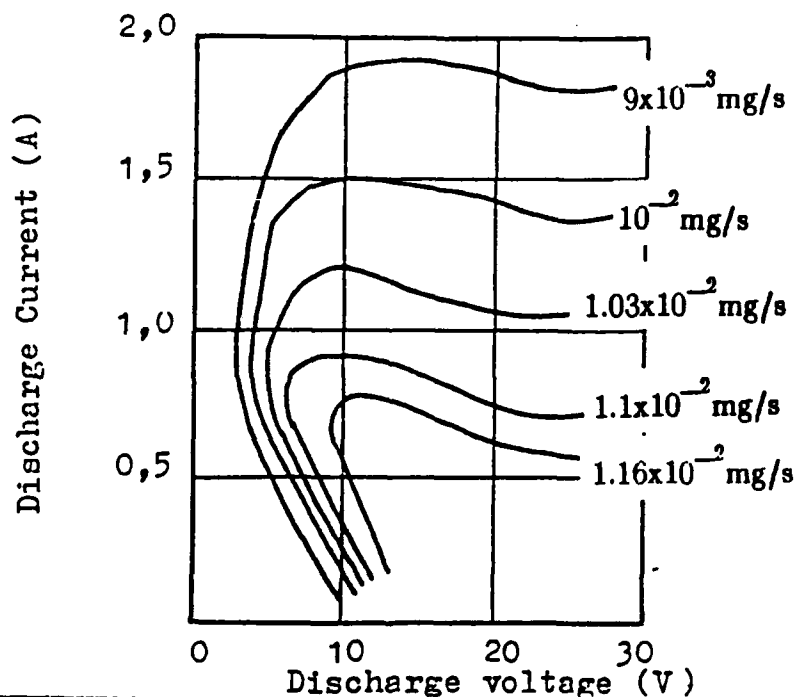


Fig. 2.6 Voltage-Ampere Discharge Characteristics of Cesium Hollow Cathode [Ref.19]

#### 4. China

Pulse ignition characteristics for a hollow cathode for an electron bombardment mercury ion thruster was presented in China in 1984. A high-voltage pulse igniter with positive pulse output of 0.1 kV – 6 kV was developed. The pulse ignition voltage of the hollow cathode was measured as a function of pulse width, pulse repeat frequency and mercury flow rate respectively. A comparison between D.C. ignition voltage and pulse ignition voltage was also made. The pulse ignition voltage dropped with the increase of the pulse width. Also, the voltage dropped as the pulse repeat frequency was increased. Fig. 2.7 shows the comparison between D.C. ignition voltage and pulse ignition voltage. Fig. 2.8 shows the relation between pulse ignition voltage and mass flow rate. [Ref. 28]

#### 5. Japan

A 10,000 hours neutralizer hollow cathode endurance test was run by the Electrotechnical Laboratory, Japan in 1984. The tested hollow cathode was fabricated with the same process as one for ETS-III(5cm mercury ion thruster). It was installed in a small vacuum chamber with a liquid nitrogen trap and a virtual anode was set before the cathode. Parametric change tests and spectral analysis were carried out every 1,000 hours. No severe degradation of the cathode was observed after the 10,000 hours operation. Change of the propellant flow rate is also negligibly small, compared with the beginning flow rate. Fig. 2.9 shows the entire test log of the cathode. [Ref. 30]

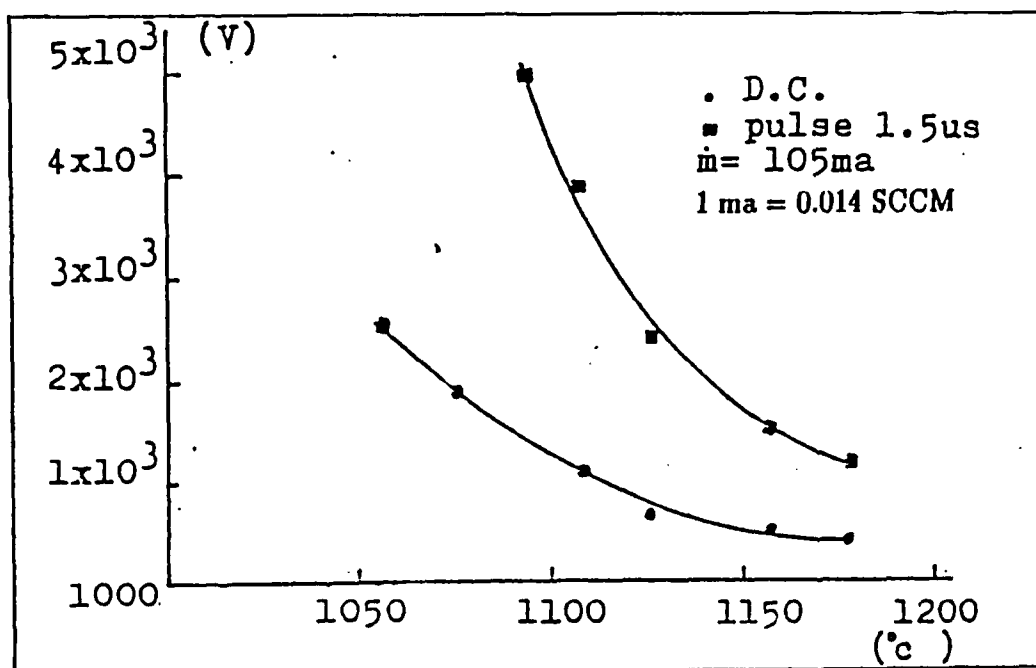


Fig. 2.7 Comparison between D.C. Ignition Voltage and Pulse Ignition Voltage [Ref.28]

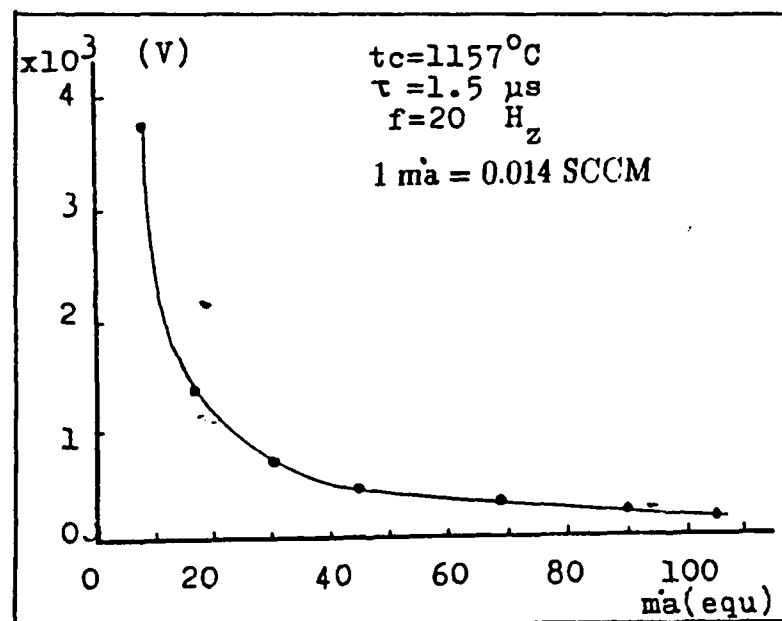


Fig. 2.8 Relation between Pulse Ignition Voltage and Mass Flow Rate [Ref. 28]

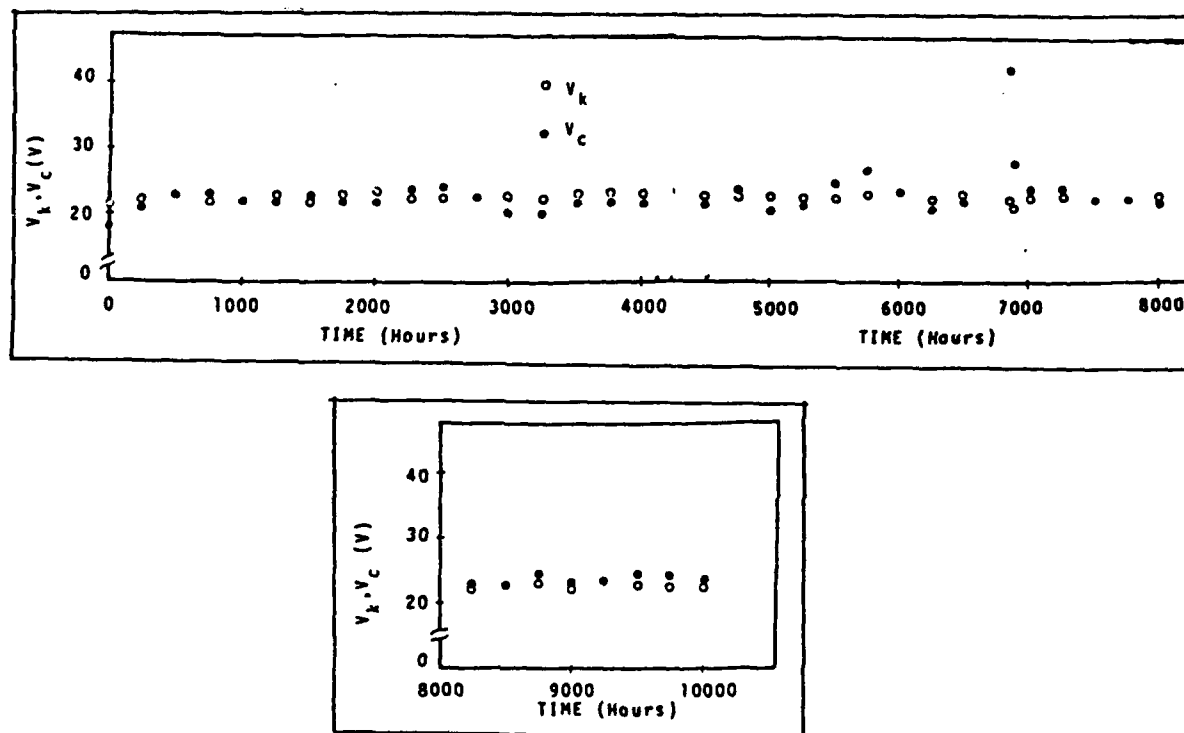


Fig. 2.9 Test Log of the Cathode [Ref. 30]

### C. HEATERLESS HOLLOW CATHODE

With inert gas (for example, Argon), the cathode heater is not needed to prevent condensation. Further, hollow cathodes in laboratory inert gas ion thrusters have been started without a hollow cathode heater by flooding the cathode during ignition. Although it has been demonstrated that reliable heaters are possible, some view them as a failure prone component which is sensitive to fabrication procedures. Ultimately, heaterless ignition of ion thruster hollow cathodes should contribute to more reliable ion thruster designs with a lower parts count.

Heaterless inert gas ion thruster hollow cathodes were investigated with the aim of reducing ion thruster complexity and increasing ion thruster reliability. Before the hollow cathode can ignite without a heater, the propellant must

breakdown electrically without a heater. (Note that "ignition" means establishing a low voltage (10 to 40 V) high current (>1 A) electrical discharge (i.e., an "arc"), while "breakdown" implies the onset of an electrical discharge in some mode (not necessarily an arc).) Thus, it is important to first understand what mechanisms govern the heaterless breakdown of propellant. In this investigation, Paschen's law served as the model of electrical breakdown.

### 1. Theory

For clearer understanding, the derivation of Paschen's law is briefly presented. The breakdown voltage is

$$V_b = \frac{B(P \cdot D)}{C + \ln(P \cdot D)} \quad (2.11)$$

where  $P$  is the pressure and  $D$  is the distance between the electrodes. Fig. 2.10 shows  $V_b$  as a function of  $(P \cdot D)$ , and the constants  $\gamma$ ,  $A$  and  $B$  for several gases are given in Table 2.1. For large values of  $(P \cdot D)$  the breakdown voltage  $V_b$  according to equation (2.11) rises nearly linearly with  $(P \cdot D)$  because the logarithmic term varies slowly. For small values of  $(P \cdot D)$  the numerator in equation (2.11) decreases linearly with decreasing  $(P \cdot D)$ , but  $\ln(P \cdot D)$  decreases faster, with result that  $V_b$  rises when  $(P \cdot D)$  is lowered. Hence there is a minimum  $V_b$  (called Paschen's minimum) whose value is found from  $dV_b/d(P \cdot D) = 0$ , viz.

$$(P \cdot D)_{\min} = (2.72/A) \ln(1 + 1/\gamma) \text{ and } (V_b)_{\min} = B(P \cdot D)_{\min} \quad (2.12)$$

It follows that, for example, the lowest breakdown voltage is to be expected for gases and cathodes for which  $B/A$  is small and  $\gamma$  is large (Fig. 2.10). Table 2.2 shows

the minimum values for a number of gases. The general trend is in agreement with equation (2.12). For instance, for a given cathode in rare gases, the constant  $A$  is often smaller and  $\gamma$  larger than in molecular gases and thus  $(P \cdot D)_{\min}$  is larger. Again  $B$  is small for the rare gases and so is  $V_b$ . [Ref. 15]

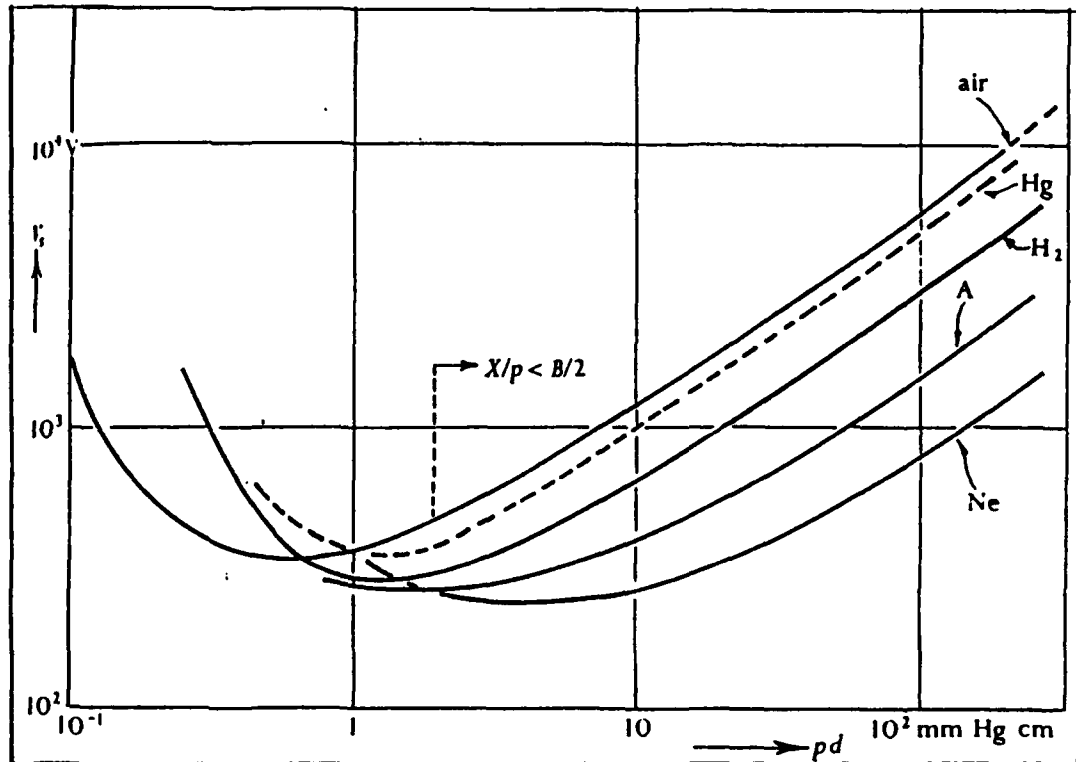


Fig. 2.10 Paschen's Law (Breakdown voltage  $v_b$  as a function of the reduced electrode distance  $P \cdot D$ ). [Ref. 15]

TABLE 2.1 VALUES OF COEFFICIENTS A AND B IN (2.11) FOR  
VARIOUS GASES. [REF. 15]

Gas	A $\frac{1}{\text{cm mm Hg}}$	B $\frac{V}{\text{cm mm Hg}}$	Range of validity X/P
N <sub>2</sub>	12	342	100-600
H <sub>2</sub>	5.4	139	20-1000
Air	15	365	100-800
CO <sub>2</sub>	20	466	500-1000
H <sub>2</sub> O	13	290	150-1000
Ar	12	180	100-600
He	3	34(25)	20-150(3-10)
Hg	20	370	200-600

TABLE 2.2 MINIMUM SPARKING POTENTIALS [REF 15]

Gas	Cathode	V <sub>min</sub> (Volts)	(P * D) <sub>min</sub> (mm Hg cm)
He	Fe	150	2.5
Ne	"	244	3
Ar	"	265	1.5
N <sub>2</sub>	"	275	0.75
O <sub>2</sub>	"	450	0.7
Air	"	330	0.57
H <sub>2</sub>	Pt	295	1.25
CO <sub>2</sub>	?	420	0.5
Hg	W	425	1.8
Hg	Fe	520	≈ 2
Hg	Hg	330	?
Na	Fe ?	335	0.04

Paschen's Law has been experimentally established for well defined P (static gases) and D (parallel plate geometry) (Fig. 2.10); however, neither criteria is satisfied in the standard hollow cathode geometry because the geometry is nonplanar and the pressures are nonstatic in the breakdown region between the cathode orifice plate and the keeper. Nevertheless, one would expect the trends to remain the same, i.e., when breakdown voltage is plotted as a function of  $P \cdot D$  for the hollow cathode, perhaps a Paschen minimum could be found near the 1 MMHG\*CM value characteristic of well defined  $P \cdot D$  cases (Fig. 2.10). Examining the standard hollow cathode under this assumption, with reasonable estimates of P and D, the  $P \cdot D$  product is seen to be well below this characteristic value ( $P \cdot D = (0.001 \text{ MMHG}) \cdot (0.15 \text{ CM}) = 0.00015 \text{ MMHG} \cdot \text{CM}$ ). Hence Paschen's law is not well suited to the conditions in a standard hollow cathode. Paschen's theory would qualitatively explain the experimental observation that for heaterless ignition of hollow cathodes high flow rates are required. Increasing the  $P \cdot D$  product by increasing P through increased flowrate brings the breakdown voltage down to the level satisfied by the open circuit voltage of the igniter supply. Demanding heaterless ignition at reasonable igniter supply voltages ( $<1 \text{ KV}$ ) implies that electrical breakdown in heaterless hollow cathodes should occur near Paschen minimum breakdown voltages, typically on the order of 200 to 400 V for most gases. (Fig. 2.10)

Under Paschen's Law, the breakdown voltage for the heaterless hollow cathode can be lowered in a number of ways (e.g., lengthening D, increasing P, "seeding" the propellant with a low ionization potential material, etc.). [Ref. 10]

## 2. Hardware

Heaterless inert gas ion thruster hollow cathodes were investigated



with the aim of reducing ion thruster complexity and increasing ion thruster reliability. One of the heaterless cathode is the design invented by Aston, 1981. [Ref.18] This design is manufactured by Spectra-Mat Inc. and is referred to in this thesis as the Spectra-Mat cathode.(Fig. 2.11) This cathode design provides an alternative to the refractory metal filament cathode. The Spectra-Mat model modifies the original design by Aston by including a tungsten dispenser. Porous tungsten with a formula of barium oxide dispersed throughout the matrix is the essential form of dispenser cathodes. The claimed performance for the Spectra-Mat hollow cathode is a starting time of approximately ten seconds after which the device is capable of emitting several amperes of electron current. Gas flow requirements are low. With argon, a flow rate of 3-5 sccm (standard cubic centimeters per minute) will support a cathode emission current level of 5-10 amperes. Lower gas flows can be used for smaller electron emission current requirements such as ion beam neutralizer applications. An inherent operating characteristic of hollow cathodes requires that the anode supply be current regulating with a compliance voltage of about 80-100 volts. The fast emission current response of the Spectra-Mat hollow cathode means that anode power supply response times less than 1 msec are required. Most transistor regulated laboratory power supplies satisfy this requirement.

There are several advantages claimed for the Spectra-Mat hollow cathode. Some of these advantages are listed here.

- Much longer cathode life. The electron emitting surface is within the hollow cathode and so is shielded from sputtering damage by the 50-100 volt ions in the ionizing plasma

- Lower power consumption and operating temperatures. This results in less undesirable substrate and process chamber heating.

— Less chance of ion beam and substrate contamination. The hollow cathode is subject to much less evaporation because of its lower operating temperatures.

A unique feature of the Spectra-Mat hollow cathode is the ability of the cathode to be placed in an idle mode where the cathode is on but no discharge chamber plasma or ion beam is being produced. This feature is especially useful in continuous operations, such as ion etching, ion sputter deposition, ion milling and ion implantation. In these applications, the ion source can be pulsed on as each new substrate is put in place. This minimizes the chamber heating and ion sputter erosion, promoting a much cleaner substrate environment. [Ref. 1]

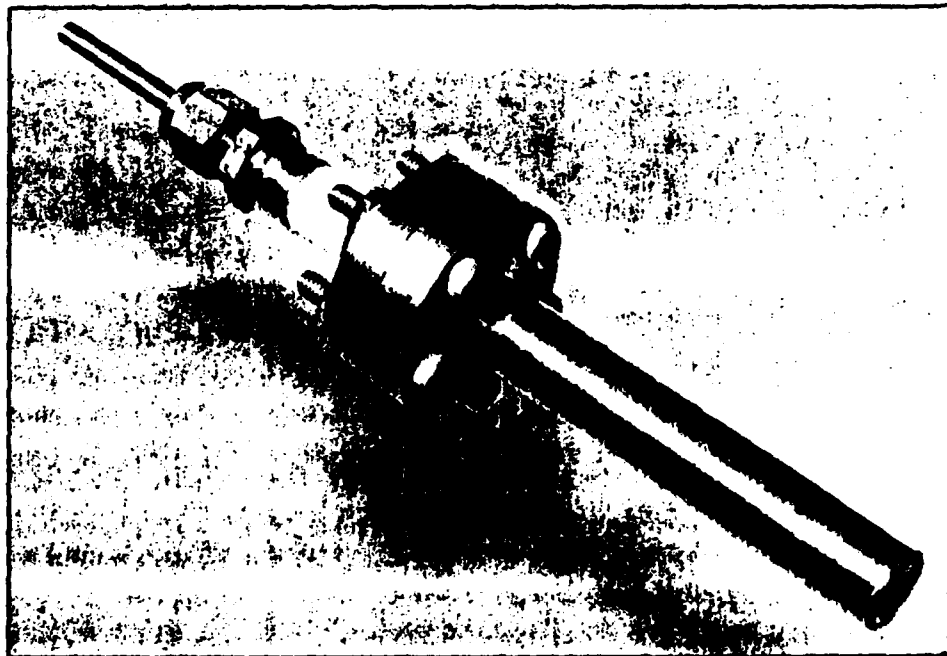


Fig. 2.11 Spectra-Mat Hollow Cathode Apparatus.

### III. EXPERIMENTAL EQUIPMENT AND PROCEDURE

#### A. EXPERIMENTAL EQUIPMENT

##### 1. Discharge Chamber

Fig.3.1 is the picture that illustrates the general experimental arrangement. There are four main components in the vacuum chamber. They are cathode, keeper, anode and Langmuir probe.

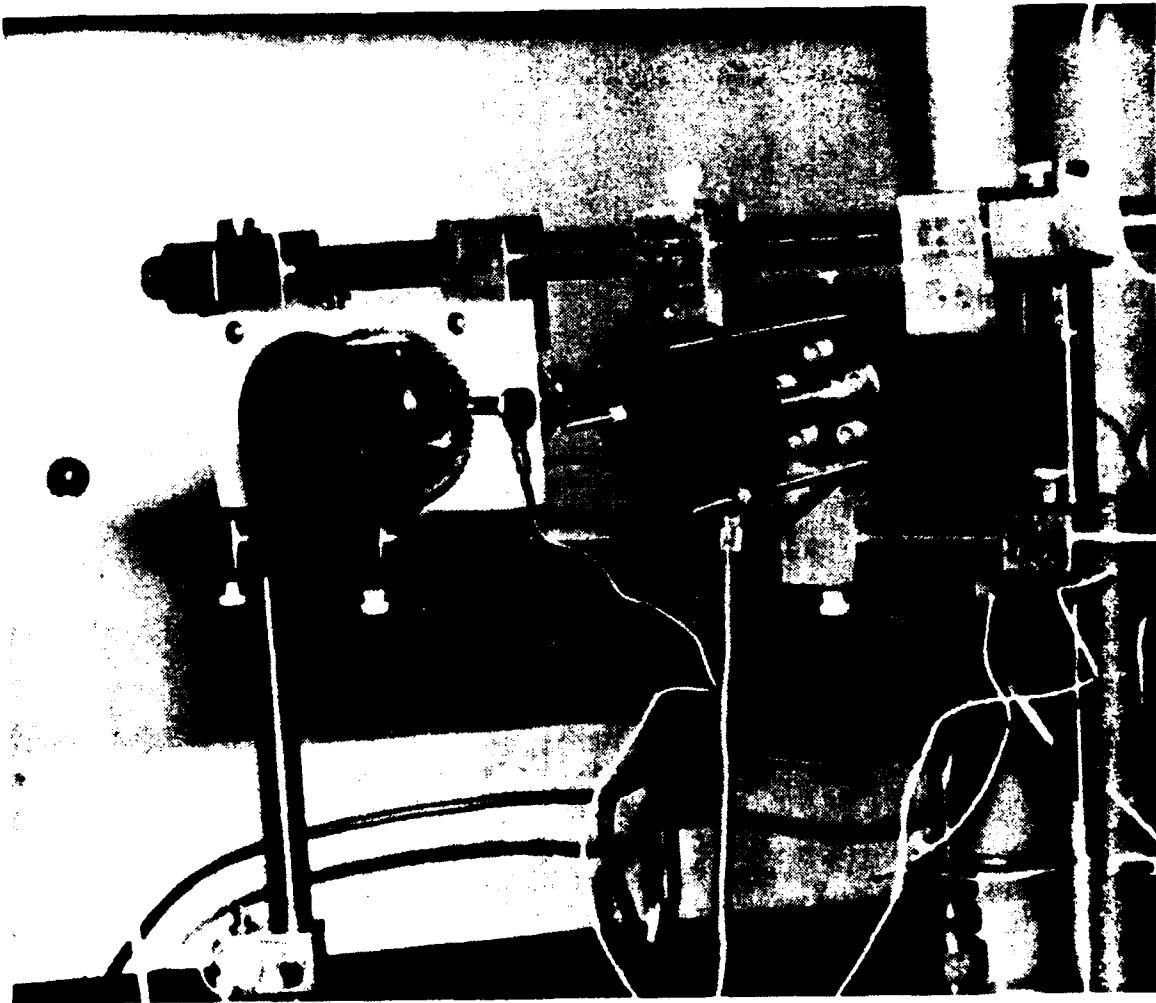


Fig. 3.1 General Experimental Arrangement.

Two hollow cathodes (a standard design manufactured by Ion-Tech and the Spectra-Mat cathode) are mounted parallel to each other. Only one cathode can be used at a time. The standard cathode was mounted so that the distance between the cathode tip and the keeper could be varied. This is the subject of the thesis by Park. [Ref.38] Both of the cathodes are connected to copper tubes by swagelock connectors and receive argon gas through these tubes. The copper tubes were disconnected in the middle and they were replaced by tygon tubing for electrical isolation. The Spectra-Mat hollow cathode has the keeper in its body, but a similar appearing external anode.

A Langmuir probe has been placed in the chamber to measure the electron temperature, electron current and plasma density. The Langmuir probe is a stainless steel ball (diameter 9.514mm) and it is connected by a thin stainless steel bar. This bar is covered with ceramic to insulate it from the plasma in the chamber.

The anode, or collector, is designed to collect the discharge current and to take the role of the electric field of the space environment. The anode is a copper grid which surrounds the inside wall of the jar.

## 2. Electrical Circuit

Fig.3-2 illustrates the electrical circuitry for the Ion-Tech(standard) hollow cathode. As expected, High voltage ( $\approx 300V$ ) is applied to start the discharge. Right after the ignition, two circuits exist. However, only a low current can flow through the very high resistor ( $110k\Omega$ ). Therefore only the low voltage, high current supply is active after the initial igniter.

Fig.3-3 illustrate the electrical circuitry for the Spectra-Mat heaterless hollow cathode.

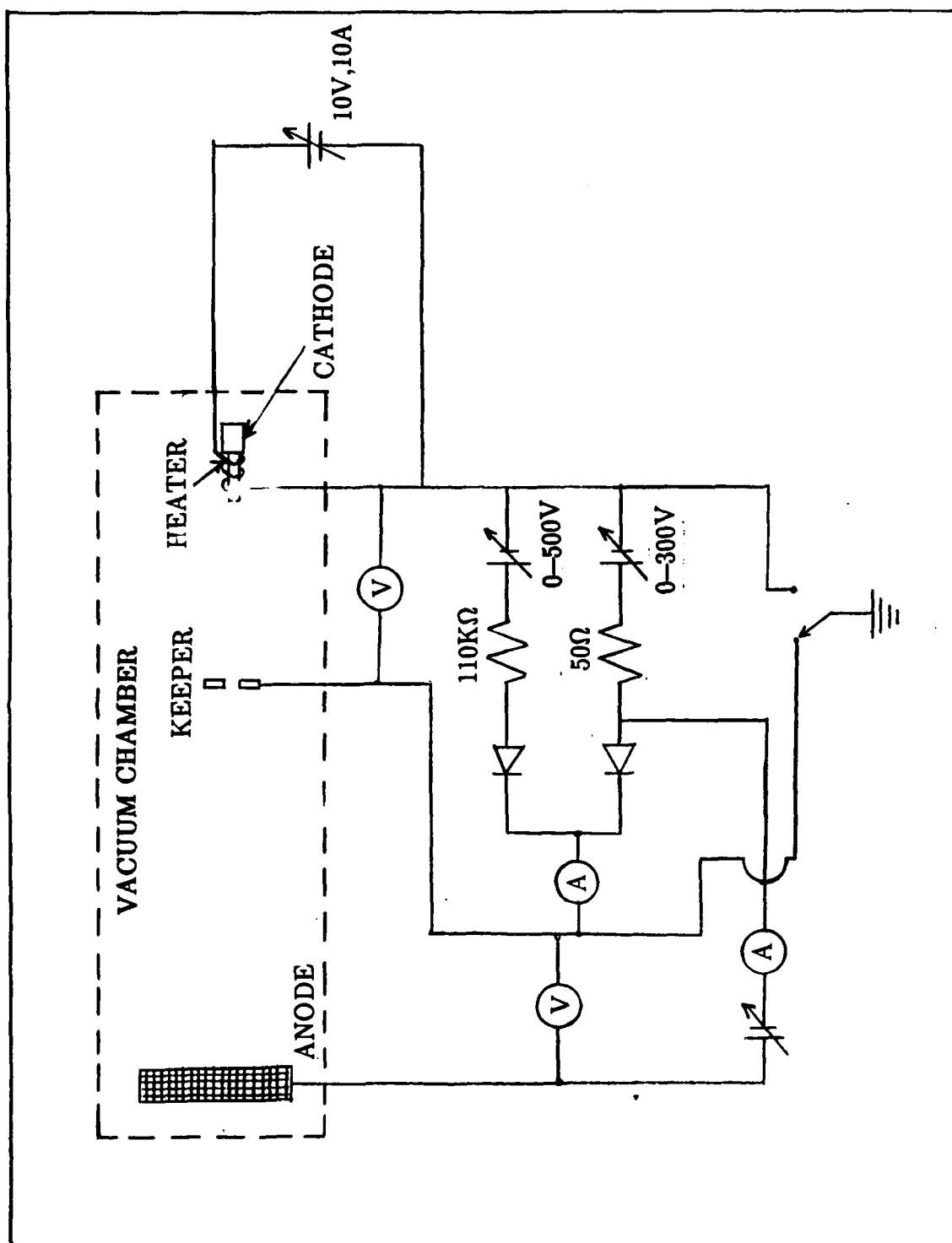


Fig. 3.2 Electrical Circuitry for the Ion-Tech Hollow Cathode.

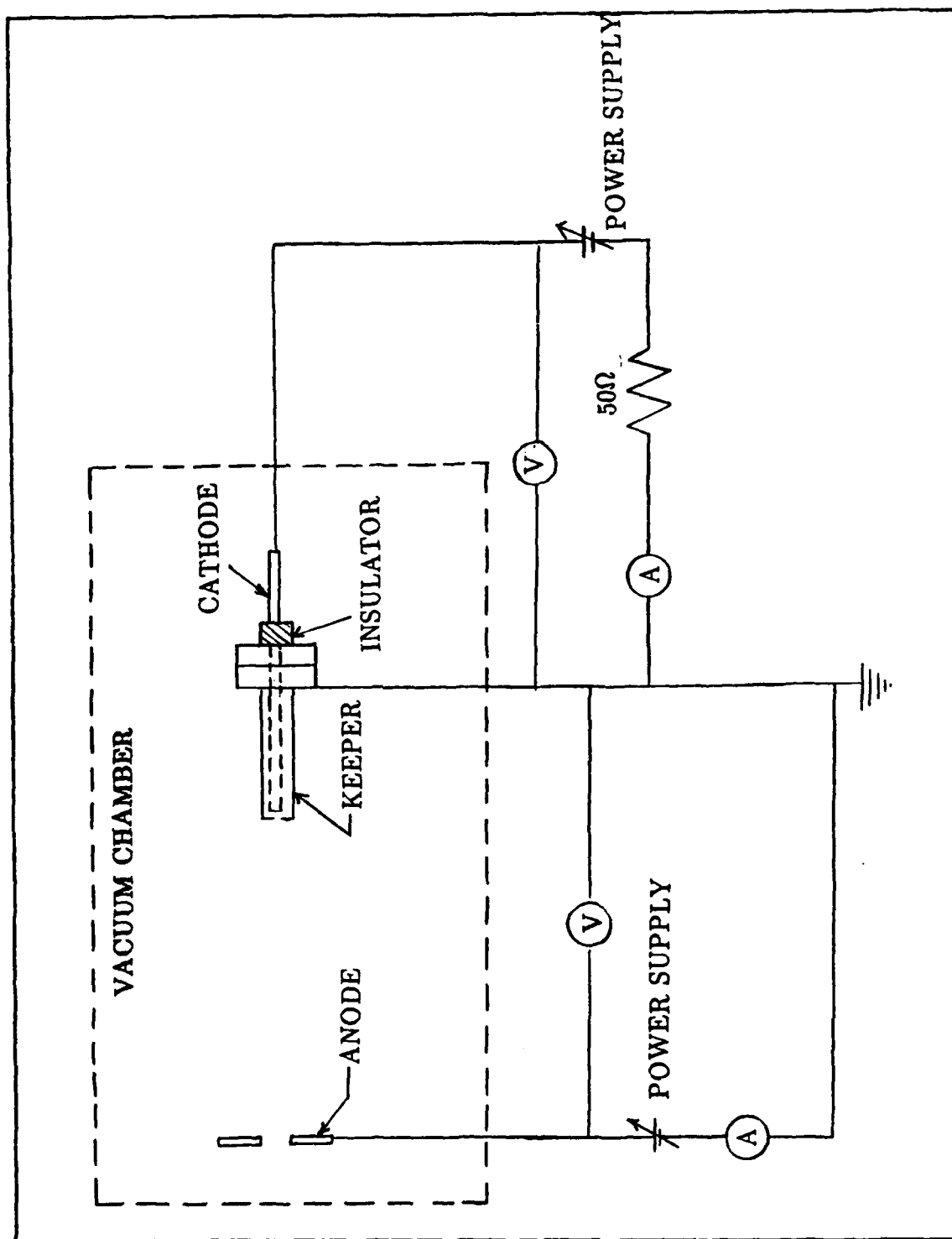


Fig. 3.3 Electrical circuitry for the Spectra-Mat Hollow Cathode

### 3. Measuring Equipment

Two Varian Type 0531 thermocouples were used to measure the pressures in the rough vacuum range and Varian 880RS ionization gauge was used to measure the high vacuum pressures.

Fluke 85 multimeter, Fluke 75 multimeter and Keithley 195A DMM were used to measure the anode to keeper current, the keeper to cathode current and keeper to cathode voltage respectively.

HP model 120B oscilloscope was usually used to watch the system noise and the plasma oscillation.

HS-10S Hasting mass flow transducer and Nall flow meter are used to measure the argon gas flow rate. (unit: SCCM—standard cubic centimeters per minute)

### 4. Vacuum System

Fig.3-4 shows the major parts of the Varian system. This vacuum system consists of two pumps. A Rotary Vane Oil-Sealed Mechanical Pump is used for rough pumping; pressure range 760 torr to  $10^{-3}$  torr. A Turbo pump is used for a high vacuum pumping; pressure range  $10^{-3}$  torr to  $10^{-8}$  torr. For this experimental system, base pressure without propellant flow is  $2.8 \times 10^{-6}$  torr with valves to the gas supply open. Fig. 3.5 shows the relationship between argon flow rate and vacuum chamber pressure. Chamber pressure increases linearly by increasing the flow rate as expected.

## B. Procedure

### 1. Vacuum System

In order to start this experiment, the Bell Jar should be evacuated to the order of  $10^{-6}$  torr.

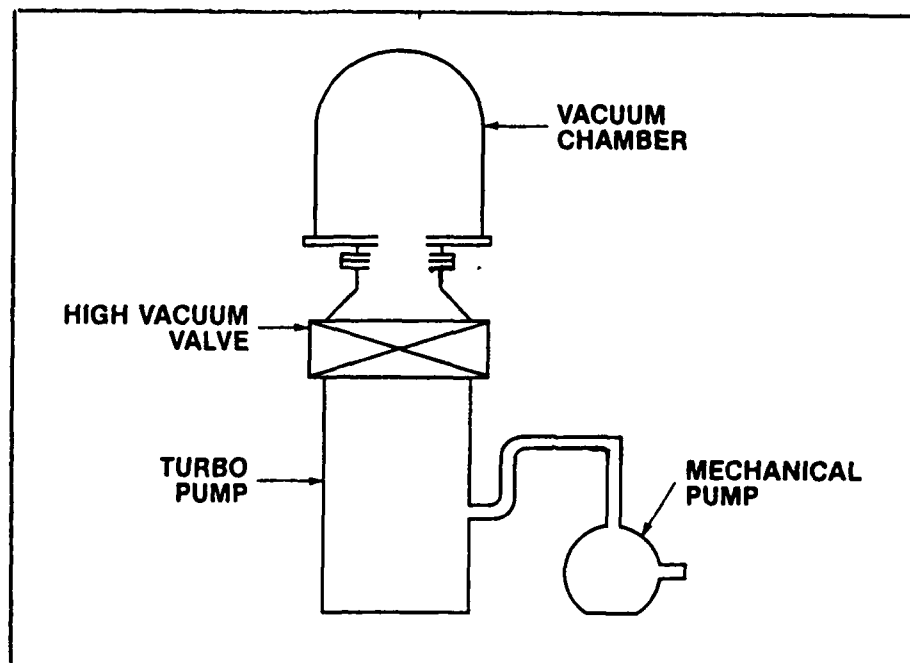


Fig. 3.4 Major Parts of Varian Vacuum System.

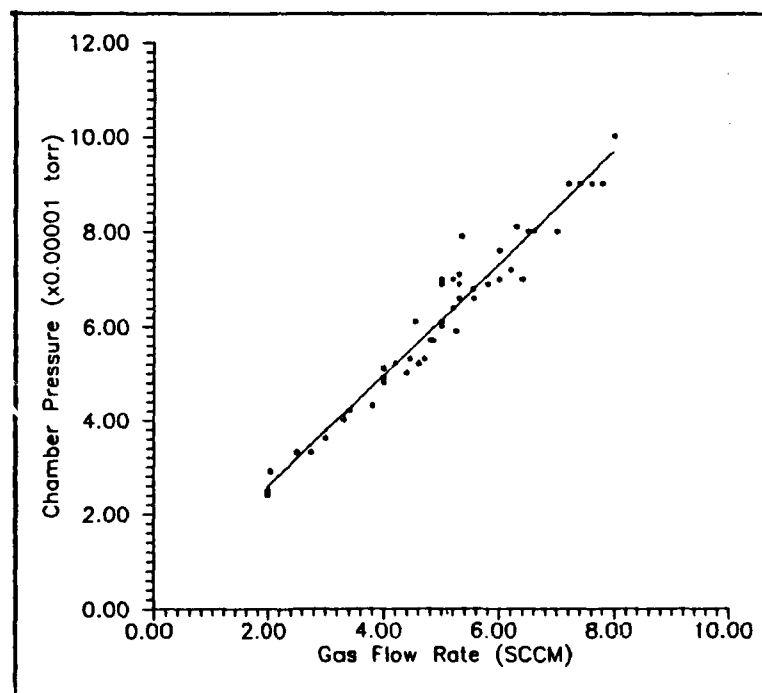


Fig. 3.5 Relation between Propellant Flow Rate and Chamber Pressure



It usually takes several hours to reach the desired pressure range of the vacuum chamber and up to 24 hours pumping to assure complete outgassing. The procedure for operating the vacuum system is as follows;

(A) Turn on the cooling water and open the nitrogen gas bottle valve (Nitrogen bottle valve is set to 2.5 – 5.0 psi as the regulated pressure)

(B) Place switch marked "Turbo Pump" to "Off" position

(C) Switch on power to turbo controller and ionization gauge

(D) Push "Start" on controller. Roughing pump should start, turbo pump should not. Let system pump down to 100 milli torr as indicated by TC2 gauge on ionization gauge panel.

(E) With controller in "Low Speed" (i.e., Low speed button depressed) Switch "Turbo Pump" switch to "On" when 100 milli torr reached

(F) "Acceleration" and "Leak" indicators will light. Both should go out and "Normal" indicator will light within 5 minutes

(G) Switch on ionization gauge to read pressure.

When cathode has been exposed to atmosphere, allow vacuum system to pump down at least overnight before attempting to start plasma.

## 2. Starting and shutting down the plasma source

### (A) Standard Hollow Cathode

(1) As mentioned above, for the initial start up (if cathode has been exposed to atmosphere) make sure the vacuum system has pumped down overnight. The gas lines should be flushed twice with argon – it takes 1–2 hours to pump out the gas lines once the argon cylinder is sealed.

(2) Set the heater current to 4A for 10 minutes. Then, increase in 1A increments to 8A waiting 10 minutes between each increase.

(3) Start the argon flow at 3–5 SCCM. Increase the heater current to 9A. Set the anode voltage to  $\approx 300V$ .

(4) Wait several minutes. (If discharge does not start, increase the flow rate to 5 or 6 SCCM. Wait again. If nothing happens, reduce flow rate back to 2.5 – 3.0 SCCM. When flow stabilizes, quickly open and close the bypass valve 1/4 turn. Do not leave the bypass valve open or the vacuum system will overload. Repeat as necessary until a stable discharge ignites.

(5) When the plasma source starts, a sudden drop in voltage and rapid increase in current will occur. When this happens, immediately reduce the heater current to 6A and adjust the flow rate to the desired level. (2 – 4 SCCM range works best)

(6) Change parameters as required. Slow changes work best. Rapid changes in current (i.e. 0.2 → 2A) may cause loss of plasma.

(7) To shut down the plasma source, Switch off the power supply and reduce the heater current slowly to 0A. (Opposite to the initiation) Allow argon gas to flow at 2 SCCM.

(8) Do not switch off vacuum system while cathode is hot. (It is best to wait at least one hour to allow complete cooling). If power loss should occur, close gate valve and shut off argon flow immediately. This will maintain a vacuum in the Bell Jar while cathode cools.

(9) To restart plasma source when plasma loss occurs while changing parameters, bring up the heater current to 9A immediately and set the propellant flow rate to 3 SCCM and wait. Discharge usually auto-starts quickly. Restarts are normally quicker and easier than the initial daily start.

**(B) Spectra-Mat Heaterless Hollow cathode**

(1) The initial stage is the same as that of the Ion-Tech cathode.

(2) Increase the flow rate to 5 SCCM.

(3) Turn on the power supply and increase the voltage slowly to 270V.

(4) Wait 30 seconds. If nothing happens quickly open and close bypass valve 1/4 turn. Do not leave bypass valve open or you will cause vacuum system to overload. If plasma still does not start, try again when pressure is stable.

(5) When the plasma source starts, a sudden drop in voltage (to  $\cong 10V$ ) and rapid increase in current (to  $\cong 1.5A$ ) will occur and voltage regulated mode changes to current regulated mode.

(6) Change parameters as required. Slow change works better. Rapid change in current may cause loss of plasma.

(7) To shut down the plasma source, decrease the current slowly to zero.(opposite to the initiation) Allow argon gas to flow at  $\cong 2$  SCCM.

## IV. EXPERIMENTAL RESULTS

The purpose of this investigation is to find the optimum parameters that make the hollow cathode initiation certainly and operation properly. Not only the continuous, long-life operation but also proper, quick and reliable starting condition is important for the hollow cathode discharge. Starting behaviors running conditions vary according to the following parameters; propellant flow rate( $\dot{m}$ ), biasing potential between cathode and keeper( $V_k$ ), cathode tip temperature( $T$ ) or heater current( $I_h$ ), keeper spacing( $D$ ) and time of turning on and off( $t$ ).

### A. STANDARD HOLLOW CATHODE

#### 1. Flow Rate Dependence

It was sufficient to increase the temperature slowly to about 1300°C (heater current 8A) and to hold it steady for about 1 hour. Discharge initiation could then be accomplished by passing a sufficient flow rate of argon through the cathode while applying a potential  $V_k$  to the keeper. From this condition, several data could be taken. At first,  $V_k$  was slowly increased at constant flow rate until discharge occurred at a voltage  $V_d$ . This process was repeated many times at different flow rates. Fig. 4.1 shows the result. From this result, as flow rate was increased,  $V_d$  became smaller, discharge occurred faster and more predictably.

#### 2. Heater (Temperature) Dependence

$V_k$  was increased at constant temperature until discharge occurred at a potential  $V_d$ . This was repeated at different heater current (temperatures). Changing the heater current was used. Fig. 4.2 shows the heater current

dependence. From Fig.4.1 and Fig. 4.2, as either(flow rate or temperature) was increased,  $V_d$  became smaller and more predictable. With the flow rate and heater current 5 SCCM and 8 A, the discharge could often be initiated at voltages as low as 40 V.

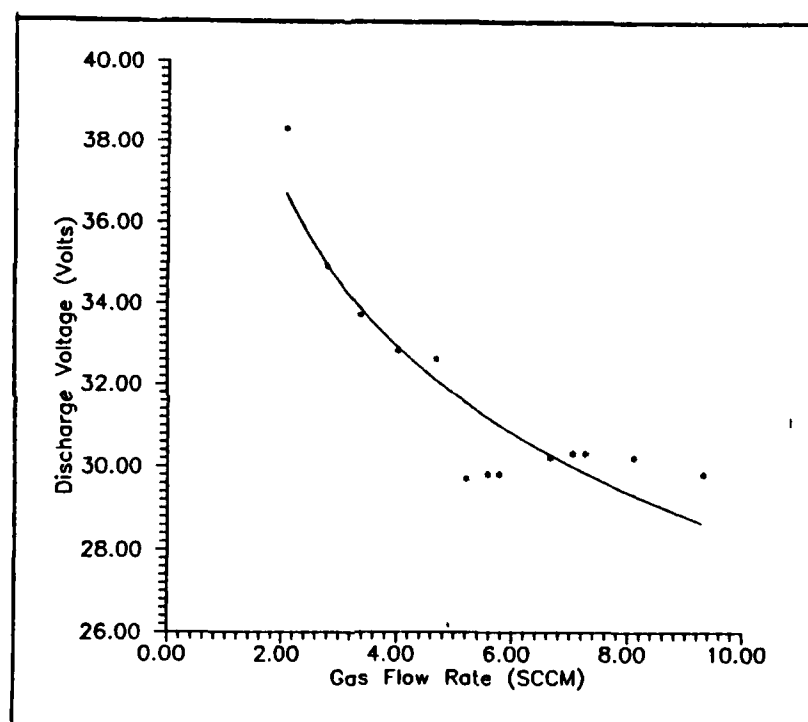


Fig. 4.1 Discharge Voltage vs Flow Rate

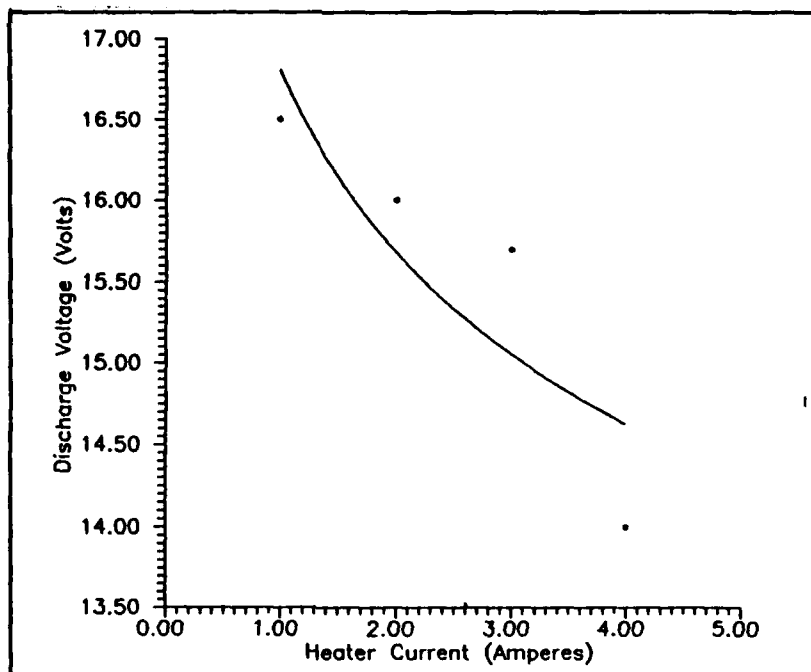


Fig. 4.2 Discharge Voltage vs Heater Current

### 3. Time Dependence

On closer examination, it was found that discharge initiation was not as unpredictable as at first thought. After the discharge had been off for several hours,  $V_d$  was generally high at given values of flow rate and temperature. In contrast, it was considerably lower if  $V_k$  was reapplied shortly after the discharge had been switched off. The time taken for the discharge to strike after application of  $V_k$  was also dependent upon the recent history of the cathode. In this experiment, the values of temperature (heater current) and flow rate were held constant, the discharge was extinguished and a known time was allowed to elapse before a fixed value of  $V_k$  was applied. At this stage, a very faint glow emerged from the cathode orifice; this was accompanied by a idle mode current of several microamperes. (Fig. 4.3) This is the thermionic emission current. The luminosity

gradually increased, as did the current, until a discontinuous rise to several hundred milliamperes indicated discharge ignition. The maximum idle mode current was approximately constant at given values of flow rate and temperature. The relatively long times involved in these phenomena suggest that chemical changes or the surface migration of barium are responsible. If the initiation mechanism as discussed in the background section is applicable, adequate thermionic emission is essential from areas close to the cathode orifice, implying that sufficient barium must be available there. Once the discharge is switched off, it would appear that barium is gradually lost from the emitting zone, so that, after reapplication of  $V_k$ , a finite time is required for replenishment. The situation is undoubtedly extremely complex, and no attempt has been made to ascertain the nature of the chemical and surface processes taking place. It would be reasonable to assume, however, that the geometry and position of the dispenser have by no means been optimized.

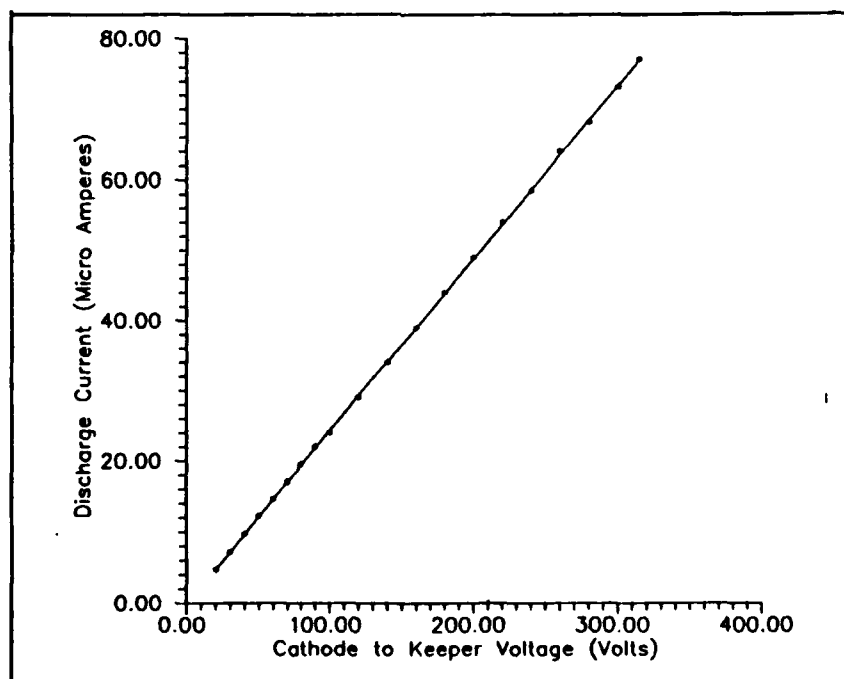


Fig. 4.3 Idle Mode Discharge Current vs Keeper Biasing Potential

## B. SPECTRA-MAT HOLLOW CATHODE

To find out the optimum parameters for Spectra-Mat hollow cathode to operate properly, similar experiments were attempted. Flow rate and biasing keeper potential were the main parameters. Unlike the standard hollow cathode, the Spectra-Mat hollow cathode does not have a heater to activate the cathode. When a sufficient biasing keeper potential ( $\cong 315\text{V}$ ) was given, a very small discharge occurred within the hollow cathode. This is the so called idle mode discharge. Idle mode discharge began in a short time ( $\leq 10$  secs). In order to extract a current, a second, outer anode must be mounted and a biasing potential applied.

### 1. Idle Mode Discharge

During this experiment, two kinds of idle mode was found, lower level and higher level. Fig. 4.4 shows these two levels of idle mode discharge for different flow rates. When the idle mode was higher level, extraction of discharge was easier. That means lower level is insufficient for activation of external discharge. To reach the higher level, hollow cathode should be turned on for several hours. That helps migration of the barium to the surface of the cathode. Idle mode discharge current also depends on the biasing keeper voltage. Fig. 4.5 shows one typical example of this dependence. Discharge current has the transition point around 295V. Above this range, the inside idle mode discharge can be seen. This idle mode discharge should be explainable by field enhanced emission. Note that this design approximately one order of magnitude higher current in idle mode. This is presumably due to the more effective fields to the cylindrical capacitor which is presented by the Spectra-Mat cathode.



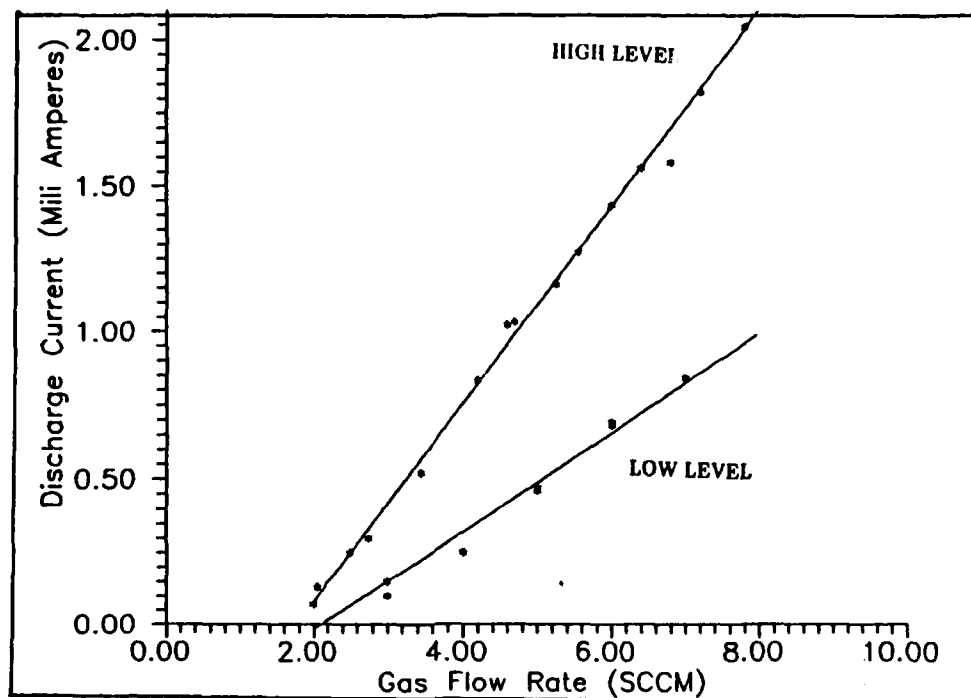


Fig. 4.4 Idle Mode Discharge for Different Flow Rate

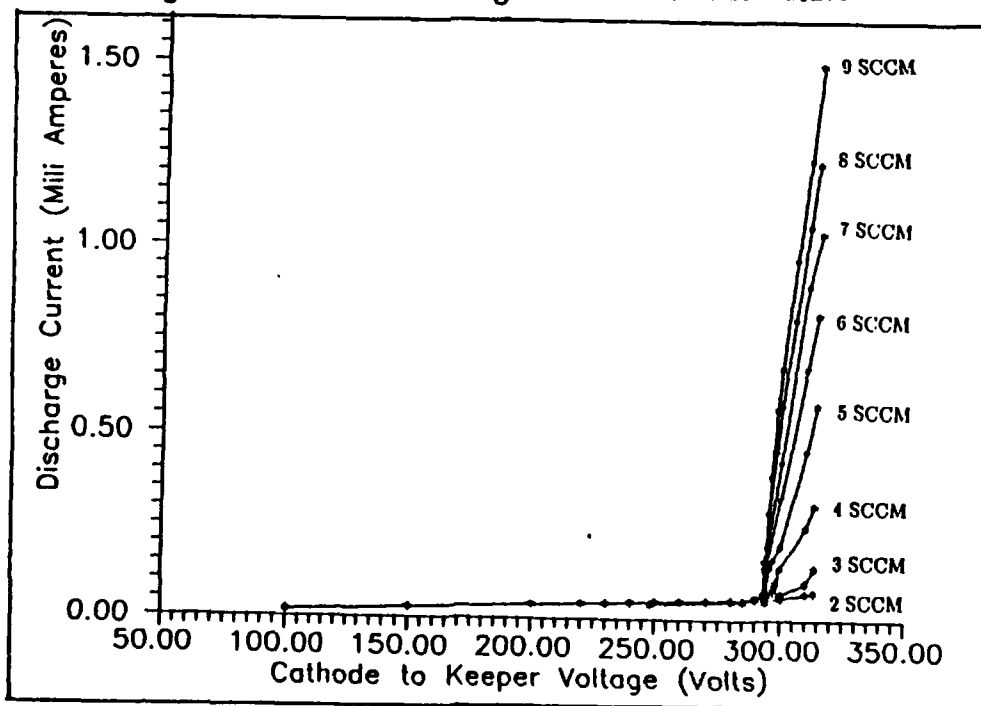


Fig. 4.5 Idle Mode Discharge Current for Different Biasing Voltage

## 2. Extraction of Discharge

Discharge extraction was unlike that found for the standard hollow cathode. If discharge extraction was easy and reliable, the Spectra-Mat hollow cathode would be highly recommended. Unfortunately, it was not easy at all. It took a long time for the first beginning attempt. Instead of the heater power supply, the Spectra-Mat hollow cathode needs another power supply to bias the anode to keeper potential. That compensate each other. Several data could be taken. The problem was that the status of the discharge was not stable and did not run long.

There were two kinds of mode for this extraction. For the first mode, the external glow was seen, but the collected discharge current was small. This is the result at the bottom of Table 4.1. This mode was somewhat stable. It lasted around 10 minutes. However, without collecting sufficient external current(1-2A), this mode is useless.

The second mode more clearly matched our expectations. Some data were taken as follows.

TABLE 4.1 DATA FOR SPECTRA-MAT CATHODE

Flow Rate (SCCM)	Internal		External	
	$V_d$ (V)	$I_i$ (A)	$V_d$ (V)	$I_e$ (A)
high	76.5	1.22	99.1	1.3
3.75	50	1.1	99	1.3
2.95	25	1.1	99	1.3
5.59	307	0.026	60.2	0.03

The range of values of discharge voltage and current is acceptable. However, the discharge fluctuated too much and the values were unpredictable. That means that

Spectra-Mat hollow cathode is not as good as a standard hollow cathode for most electron and ion emission purposes.

### 3. Discharge Failure

In the beginning of these experiments with the original Spectra-Mat cathode, the discharge was very difficult to start. When the flow rate was increased to a very high value, ( $>10$  SCCM), the chamber pressure increased to the order of  $10^{-3}$  torr, the discharge would start momentarily. The status was very unstable. Ultimately, the cathode was destroyed by overheating and arcing. There seems to be three possible reasons for the discharge failure.

First, the cathode had been exposed to the atmosphere for too long time. The hollow cathode might have been contaminated by too much water vapor, dust, oil, etc during this period. To prevent this kind of problem, mechanical work should've been finished completely and checked several times before opening the cathode shipping containers. The hollow cathode should be stored in vacuum chamber when not in use.

A second possibility of the problem is surface damage. During the initial attempts at ignition, both flow rate and biasing potential between cathode and keeper were too high. The flow rate was increased because the discharge started in only that condition. That might cause the surface damage and too much consumption of barium oxide. Further operations should have been attempted at lower flow rates, or in idle mode.

A third possible reason for the discharge failure is manufacturing flaws. The cathode might have had uneven surfaces from the beginning. It was observed that the discharge location was not always at the front of the cathode tip. Sometimes discharge occurred around 2-3 cm back from the cathode tip. Fig. 4.6

and Fig. 4.7 shows the damaged cathode surface spot and broken part of ceramic insulator respectively. The damaged spot is the place where the discharge occurred. This is unexpected and the main reason for the ultimate discharge failure.

Fig.4.8 is a detailed diagram of disassembled Spectra-Mat hollow cathode. This old cathode was disassembled after discharge failure for better understanding of the geometrical structure. That was very helpful for understanding the inner structure of the cathode. After several other attempts to recover the cathode operation, barium oxide was recoated over the surface of the cathode tip. Liquid barium oxide was used for this work. It helped the discharge, but the results were erratic. One outer anode was mounted in front of the cathode tip. Biasing the external voltage helped the bright ignition of discharge. The cathode acted like a standard hollow cathode. Biasing voltage was high.( $\approx 190V$ ) Still unstable discharge and even discharge failure happened because of uneven coating of barium oxide and the damaged surface. The results presented above were obtained with a second cathode obtained near the end of the research period. As noted, it was also difficult to operate, though the experience gained in the initial experiments helped.

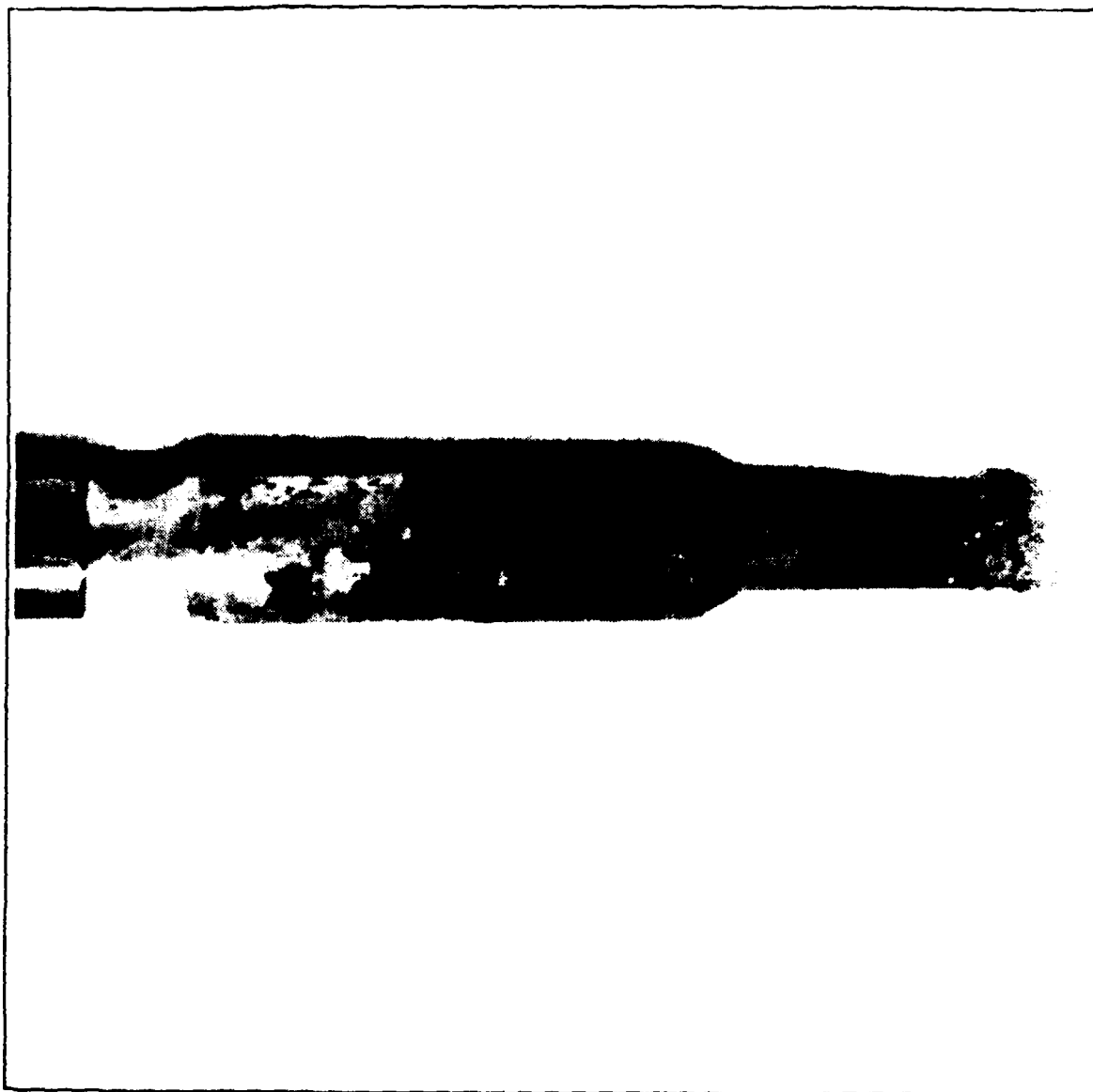


**Fig. 4.6 Picture of Damaged Cathode Surface**



**Fig. 4.7 Broken Tip of Ceramic Insulator**

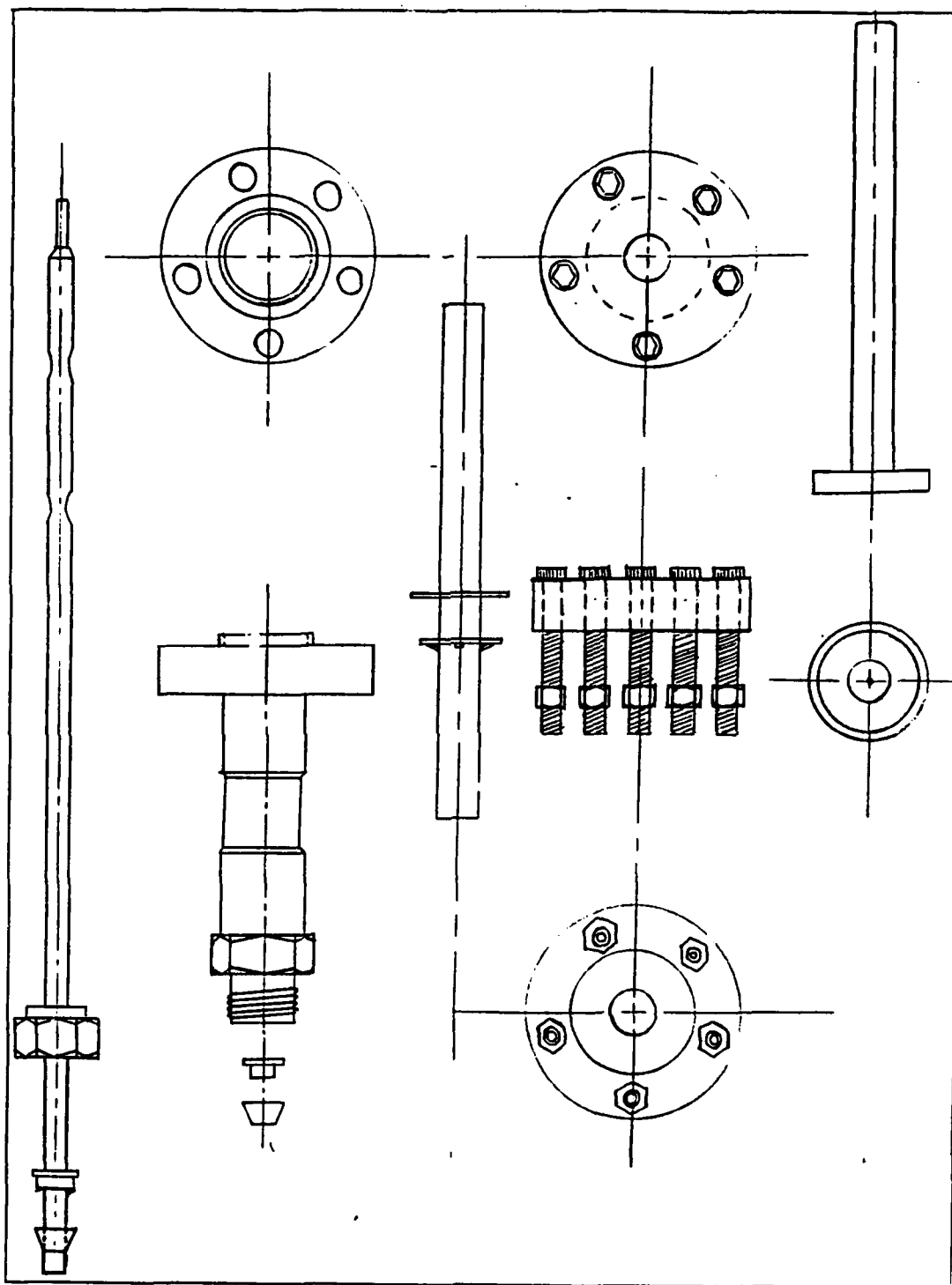


Fig. 4.8 Detailed Diagram of Disassembled Spectra-Mat Hollow Cathode

## V. CONCLUSION

Extensive investigations of the starting behaviors and parametric characteristics of two (standard and Spectra-Mat) hollow cathode designs have shown how the ignition and operation are dependent on propellant flow rate, cathode tip temperature (for standard hollow cathode), biasing potential, geometry, and the availability of a low work function material like barium oxide. As temperature or flow rate are increased, the maximum value and width of this voltage range both decrease until, at high values, starting is reproducible at potentials often below 40 volts. This behavior appears to be strongly influenced by the site and rate of dispensation of the low work function material.

For the Spectra-Mat hollow cathode, idle mode discharge occurred right after (within 10 seconds) applying a voltage of  $\approx 315$  volts. For the discharge extraction, an external anode should be mounted and 50 – 100 volts anode to keeper biasing potential should be applied. Discharge extraction is possible, but, the condition was so erratic and the values of data were unpredictable. For these reasons, Spectra-Mat hollow cathode is not highly recommended for all electron emission purposes.



## REFERENCES

1. Kim Gunther, "Hollow Cathode Plasma Source" ( Spectra-Mat Hollow Cathode Manual ), Spectra-Mat Inc., Watsonville, California
2. Aston, Graeme, "Summary Abstract: A Hollow Cathode for Ion Beam Processing Plasma Sources", Jet Propulsion Laboratory, California Institute of Technology, Pasadena, California 91109
3. Daniel E. Siegfried and Paul J. Wilbur, "An Investigation of Mercury Hollow Cathode Phenomena", Colorado State University, Fort Collins, Colorado
4. Daniel E. Siegfried and Paul J. Wilbur, "Studies on an Experimental Quartz Tube Hollow Cathode", Colorado State University, Fort Collins, Colorado
5. C.M. Philips and D.G. Fearn, "Recent Hollow Cathode Investigations at the Royal Aircraft Establishment", Royal Aircraft Establishment, Farnborough, Hampshire, England
6. D.G. Fearn, Angela S. Cox and D.R. Moffitt, "An Investigation of the Initiation of Hollow Cathode Discharges"
7. Daniel E. Siegfried, "A Phenomenological Model Describing Orificed, Hollow Cathode Operation"
8. Daniel E. Siegfried and Paul J. Wilbur, "A Model for Mercury Orificed Hollow Cathodes: Theory and Experiment", Colorado State University, Fort Collins, Colorado
9. Daniel E. Siegfried "Xenon and Argon Hollow Cathode Research", Colorado State University, Fort Collins, Colorado
10. M.F. Shatz, "Heaterless Ignition of Inert Gas Ion Thruster Hollow Cathodes", National Aeronautics and Space Administration, Lewis Research Center, Cleveland, Ohio
11. William D. Deiniger, Graeme Aston, and Lewis C. Pless, "Hollow Cathode Plasma Source for Active Spacecraft Charge Control", Jet Propulsion Laboratory, California Institute of Technology, Pasadena, California
12. Graeme Aston, "Hollow Cathode Startup Using a Microplasma Discharge", Sr. Engineer Electric Propulsion and Advanced Concepts Group, Jet Propulsion Laboratory, Pasadena, California
13. D.G. Pearn and C.M. Philip, "An Investigation of Physical Processes in a Hollow Cathode Discharge", Space Department, Royal Aircraft Establishment, Farnborough, Hampshire, England

14. C.M. Philip, "A Study of Hollow Cathode Discharge Characteristics", Royal Aircraft Establishment, Farnborough, Hampshire, England
15. Alfred von Engel, "Ionized Gases", Keble College, Oxford, England
16. Cobine, J.D., "Gaseous Conductors—Theory and Engineering Applications", 1st ed., Dover Publications, Inc., New York, 1958, chps. 5, 8, 9.
17. V.K. Rawlin and E.V. Pawlik, "A Mercury Plasma—Bridge Neutralizer", NASA Lewis Research Center, Cleveland, Ohio
18. Aston, G., "Hollow Cathode Apparatus" NASA Pasadena Office, CA. 1981
19. Maslyany N.V., Pridantzev V.F., Prisyakov V.F., Khitko A.V., "Parametric Investigations of the Hollow Cathodes for Ion Thrusters", Dnepropetrovsk State University, U.S.S.R.
20. C.M. Philip and M.O. Woods, "Some Investigations of Hollow Cathodes with Porous Dispensers", Space Department, Royal Aircraft Establishment, Farnborough, Hampshire, England
21. K. Groh and S. Walther, "Neutralizer Investigations: Performance Mapping, Position Optimization, Durability Tests". 1st Institute of Physics, University of Giessen, FRG
22. G.L. Davis (CML, Mullard, Mitcham, Surrey), D.G. Fearn (RAE, Farnborough, Hants), "The Detailed Examination of Hollow Cathodes Following Extensive Life Testing"
23. D. Newson, M.G. Charlton, G.L. Davis, "Starting Behaviours of Hollow Cathodes including Multiple Starts", CML Mullard, Mitcham, England
24. M.G. Charlton, G.L. Davis, D. Newson, "Investigations on Hollow Cathodes for Ion Thrusters", Mullard, Mitcham, Central Materials Laboratory
25. D.G. Fearn, "The Operation of Hollow Cathodes under Conditions Suitable for Ion Beam Neutralization", Space Department, Royal Aircraft Establishment, Farnborough, Hampshire, England
26. D.G. Fearn and T.N. Williams, "The Behavior of Hollow Cathodes During Long-Term Testing in a 10cm Ion Thruster and in a Diode Discharge System", Space Department, Royal Aircraft Establishment, Farnborough, Hampshire, England
27. S.E. Walther, K.H. Groh and H.W. Loeb, "Experimental and Theoretical Investigations of the Gissen Neutralizer System", Gissen University, Gissen, FRG
28. Chang Shi-liang, Hu Yong-nian, Hong Huai-yen, Sun Yu-zhu, Ren Ni, Chai Xiao-ming, "Hollow Cathode for Electron Bombardment Mercury Ion Thruster Pulse Ignition Characteristics", Lanzhou Institute of Physics, China

29. Y. Nakamura and K. Miyasaki (National Aerospace Laboratory, Chofu, Tokyo, Japan), S. Kitamura and K. Nitta (National Space Development Agency, Tokyo, Japan), "Long Time Operation Test of Engineering model of ETS-III Ion Thruster"
30. Isao Kudo, Kazuo Machida and Yoshitsugu Toda, "10,000-Hours Neutralizer Hollow Cathode Endurance Test", Electrotechnical Laboratory, Ibaraki, Japan
31. John D. Williams "Investigation of a Hollow Cathode Failure", NASA Advanced Electric Propulsion Research 1988, p39-45
32. John D. Williams, Paul J. Wilbur, "Space Plasma Contactor Research", NASA Plasma Contactor Research 1988 p1-27
33. John D. Williams, Paul J. Wilbur, "Plasma Contacting; An Enabling Technology", Colorado State University, Fort Collins, Colorado
34. John D. Williams, Paul J. Wilbur, "Ground-Based Tests of Hollow Cathode Plasma Contactors", Colorado State University, Fort Collins, CO 80523
35. J.W. Ward, H.J. King, "Mercury Hollow Cathode Plasma Bridge Neutralizers", Hughes Research Laboratories, Malibu, California
36. David F. Hall, Robert F. Kemp, Haywood Shelton, "Mercury Discharge Devices and Technology", TRW Systems Group, Redondo Beach, California
37. J. Thewlis, "Encyclopaedic Dictionary of Physics", Vol. 6, P 414.
38. Park, Young-Cheol, "Hollow Cathode Plasma Source Characteristics", Master's Thesis, Naval Postgraduate School, Monterey, CA

# INITIAL DISTRIBUTION LIST

		No. Copies
1.	Defense Technical Information Center Cameron Station Alexandria, VA 22304-6145	2
2.	Library, Code 0142 Naval Postgraduate School Monterey, CA 93943-5002	2
3.	Physics Library Code 61 Department of Physics Naval Postgraduate School Monterey, CA 93943-5000	1
4.	Department Chairman, Code 61 WH Department of Physics Naval Postgraduate School Monterey, CA 93943-5000	1
5.	Professor R.C. Olsen Code 61 OS Department of Physics Naval Postgraduate School Monterey, CA 93943-5000	10
6.	Professor S. Gnanalingum Code 61 GM Department of Physics Naval Postgraduate School Monterey, CA 93943-5000	1
7.	Maj. Han, Hwang-Jin Postal Code 134-00 Song-Pa Gu, Ga-Rak Dong, Ga-Rak APT 59 Dong 401 Ho Seoul, Republic of Korea	5
8.	Maj. Kim, Jong-Ryul Postal Code 500-00 Book-Gu, Du-Am Dong, 874-14 Kwang-Ju, Republic of Korea	1
9.	Maj. Yoon, Sang-Il Postal Code 138-150 Gang-Dong Gu, Bang-I Dong, Sam-Ik APT 201-1103 Seoul, Republic of Korea	1

- |     |   |   |
|-----|---|---|
| 10. | Maj. Seo, Yong-Seok<br>SMC 1448, Naval Postgraduate School<br>Monterey, CA 93943                                | 1 |
| 11. | Maj. Jin, Won-Tae<br>SMC 1737, Naval Postgraduate School<br>Monterey, CA 93943                                  | 1 |
| 12. | Maj. Ryu, Joong-Keun<br>SMC 1499, Naval Postgraduate School<br>Monterey, CA 93943                               | 1 |
| 13. | Cpt. Song, Tae-Ik<br>SMC 2686, Naval Postgraduate School<br>Monterey, CA 93943                                  | 1 |
| 14. | Cpt. Park, Jeong-Hyun<br>SMC 1818, Naval Postgraduate School<br>Monterey, CA 93943                              | 1 |
| 15. | Cpt. Ryu, Jong-Soo<br>SMC 2039, Naval Postgraduate School<br>Monterey, CA 93943                                 | 1 |
| 16. | Library, P.O. Box 2<br>Korea Military Academy<br>Do-Bong Gu, Gong-Neung Dong 556-21<br>Seoul, Republic of Korea | 1 |